TABLE OF CONTENTS

NASA Contractor Report 3173

A New Approach to the Solution of Large, Full Matrix Equations - A Two-Dimensional Potential Flow Feasibility Study

R. M. James and R. W. Clark

CONTRACT NAS1-14892
SEPTEMBER 1979

NASA

NASA Contractor Report 3173

A New Approach to the Solution of Large, Full Matrix Equations - A Two-Dimensional Potential Flow Feasibility Study

R. M. James and R. W. Clark
Douglas Aircraft Company
Long Beach, California

Prepared for
Langley Research Center
under Contract NAS1-14892

National Aeronautics
and Space Administration

**Scientific and Technical
Information Branch**

1979

Blank Page

TABLE OF CONTENTS

Blank Page

SUMMARY

This report presents a new approach to the solution of matrix problems resulting from integral equations of mathematical physics. Based on the inherent smoothness in such equations, the problem is reformulated using a set of orthogonal basis vectors leading to an equivalent coefficient problem which can be of lower order without significantly impairing the accuracy of the solution. This approach has been evaluated using a two-dimensional Neumann problem describing the inviscid, incompressible flow over an airfoil. Two different kinds of mode functions have been investigated, namely eigenvector series and Fourier series. The first method has the disadvantage that the calculation of each eigenvector is a time-consuming process, and the results obtained do not indicate that this is offset by the need to use only a small proportion of the eigenvectors. On the other hand, the Fourier method is attractive since all of the expansion coefficients can be calculated very rapidly using the Fast Fourier Transform algorithm. The method developed here uses all of these coefficients in an approximate method which exploits the known structure of the transformed coefficient matrix and very promising results for the flow over a realistic airfoil are obtained. The mode-function method is aimed at reducing the computer time for the solution of the equations for large three-dimensional cases. On the basis of the results presented here, it is shown that an order of magnitude reduction in this computer time can be expected for such problems as compared with the time for a direct matrix solution.

1.0 INTRODUCTION

1.1 General Background

The result of the discretization of the governing integral equation for many physical problems is a large system of linear simultaneous equations. Such systems are usually highly "nonrandom" since the original physical problem generally possesses a smoothly varying bahavior away from isolated singular regions. This is particularly true of the integral equations of many aerodynamic flow problems where the complexity comes from the geometry and a large number of points must be used to represent this adequately. This large number of points leads to a smoothly varying local behavior of the discrete quantities, but it also leads to the high computing costs associated with such calculations. For m simultaneous equations, the computing time required for a direct solution is proportional to $m^3/3$ while that required for an iterative method is pm^2 where p is the number of iterations required to obtain a fully converged solution. On the other hand, the central thesis of the mode-function approach presented here is that, for problems of this kind, advantage can be taken of the locally smooth character by replacing such a matrix equation with a related coefficient problem for certain preselected mode functions. Since a smooth function can, in general, be represented adequately in terms of a relatively small number of such functions, the size of the coefficient matrix can be significantly smaller than that of the original problem without seriously affecting the accuracy.

One problem which is of great practical significance is the calculation of the internal or external, inviscid, incompressible flow about a given shape. This is the classical boundary-value problem for Laplace's equation with a well-established mathematical pedigree (the Neumann problem) which leads to an integral equation of the second kind. "Panel methods" which provide a numerical solution of this problem have been used for a number of years for aircraft design both in the United States and in Europe. The main difficulty associated with their use is the cost incurred both in terms of the labor involved in the preparation of the input data and the computational effort involved in the solution of the resulting equations. The reduction of this computation time is, therefore, a

primary aim of the mode-function concept although it should be emphasized that the method presented here is applicable to the solution of any matrix problem, provided that the matrix possesses a dominant diagonal. The panel method developed at Douglas Aircraft Company is based on a source distribution and the associated influence matrix does possess a dominant diagonal. This problem is, therefore, particularly suited to the mode-function approach and so it has been used as the basis for most of the results presented here.

A study of the application of the mode-function method to two-dimensional Neumann problems has been undertaken although the main practical application of the techniques would be in three-dimensional calculations for which the computation times are significant. However, this present study demonstrates the validity of the mode-function concept while providing a guide to the reductions in computing time which can be expected for three-dimensional calculations. This work is also highly relevant to three-dimensional problems since, as suggested in section 6, the fitting of a large matrix associated with a complex three-dimensional configuration would be undertaken in smaller blocks corresponding to two-dimensional sections. The operation count presented in section 6.2 indicates that a three-dimensional mode-function method could offer significant savings in computer time compared with a direct matrix solution method.

Before proceeding with an outline of the theoretical basis of the mode-function approach, it will, however, be worthwhile to discuss the principal features of the panel method developed at Douglas Aircraft Company.

1.2 The Hess Panel Method

The low-speed flight regime occupies a special place in the field of aerodynamics; first because it is the one regime in which all vehicles must operate, and second because only at low speed is the governing flow equation linear (Laplace's equation) so that powerful flow-calculation techniques can be employed. In particular, the problem can be formulated as an integral equation for a certain singularity distribution over the surface of the body about which flow is to be computed (ref. 1). This procedure owes its great efficiency to the fact that the domain of calculation can be restricted to the body surface, i.e., calculations need not be performed in the field of flow. In three-dimensional problems the

numerical implementations of this procedure have represented the body surface by a large number of small four-sided surface elements or "panels" and thus have come to be called "panel methods." In the Hess version, these panels are placed on the actual body surface. This renders the method numerically "exact" and applicable to any arbitrary body. Some alternative formulations place panels interior to the body, e.g., on the mean surface of a wing. These latter methods are applicable only to a restricted class of bodies.

The above-described method of approximating a three-dimensional body is shown in figure 1. On each element, a control point is selected where the boundary condition of zero normal velocity is to be applied and where surface velocities are ultimately calculated. A "matrix of influence coefficients" is then calculated. This consists of the complete set of velocities induced by the elements on each others' control points for unit values of all singularity strengths. The integral equation that expresses the zero normal-velocity boundary condition is then approximated by a set of linear algebraic equations for the values of the singularity strengths on the surface elements. In lifting cases, the Kutta condition along the trailing edge yields a small number of additional equations. The order of the "matrix of influence coefficients" and the order of the coefficient matrix of the linear equations are both equal to the number of elements used to approximate the body (or nearly equal, depending on details of the numerical procedure). In the basic form of the method, (ref. 2) the surface elements are plane quadrilateral "panels," and each singularity strength is assumed to be constant over each element — a step function from element to element. The two time-consuming parts of the computing task are the calculation of the "matrix of influence coefficients" and the solution of the resulting linear equations. The relative importance of these two tasks depends on the body considered, the element number and the type of numerical technique employed. However, as a general rule, for complicated bodies which require very large numbers of panels, the solution of the linear equations is the harder task.

The Hess three-dimensional panel method in both its lifting (ref. 2) and nonlifting (ref. 3) versions has been distributed very widely to various government agencies, industrial concerns and universities. In general, very satisfactory results have been obtained. Probably the principal disadvantage of this or any

three-dimensional panel method is the expense of running each case. For a complete aircraft configuration, a very large number of panels is required to adequately represent the geometry, and it is expensive both to generate the necessary geometric input data and to solve the resulting system of equations. A major reduction of the time for the preparation of the input data has been achieved by the automatic geometry handling programs developed by Halsey (ref. 4). This report is concerned with the second problem, that of reducing the computing cost of the matrix solution.

1.3 The Mode Function Approach

Having outlined the panel method to which the new approach is directed, a more detailed presentation of the mode-function theory can now be given. The fundamental assumption on which it is based is that both the singularity strength and the elements of the influence matrix must necessarily be slowly varying functions of position on the body surface. Therefore, their values on adjacent panels cannot be very different, so that solving the complete set of linear equations in which every unknown is assumed to be independent is wasteful in the sense that not all of the available information is being used. In the original problem, neighboring quantities are not in any sense independent. The mode-function method, therefore, seeks to fit the matrix and the singularity distribution to account for their continuity and dependency. The new problem becomes that of determining the "strength coefficients" of the chosen mode functions. Since, for example, a relatively small number of Fourier coefficients will contain as much information as a larger number of data points, this coefficient problem can be of much lower order than the original problem.

Two basic kinds of fit have been investigated based on Fourier series and on eigenfunction expansions. While the eigenfunction method appears to offer the advantage of using mode functions specifically related to the individual problem, they have the disadvantage that their calculation is a time-consuming process. Their use would, therefore, only be justified if accurate solutions could be obtained in terms of a very small number of functions and the results presented here indicate that this is not achieved in practice. On the other hand, the use of Fourier series is attractive since these functions are well understood and the use of the Fast Fourier Transform (FFT) algorithm offers an

extremely efficient way of calculating all of the coefficients for a given function. The details of the application of each of these methods will be presented in the next section and some results bearing out these statements will be presented in section 3. However, before proceeding to that there are a few general points on the application of the mode-function method to two- and three-dimensional Neumann problems which should be discussed.

The basic integral equation for the source distribution on a three-dimensional nonlifting body takes the form (ref. 2)

$$\sigma(p) - \iint_S \sigma(q)K(p,q)dS = -\vec{n}(p) \cdot \vec{V}_\infty \tag{1}$$

where $\sigma(p)$ is the unknown source density at a point p on the body surface S. The kernel function $K(p,q)$ represents the negative of the normal velocity induced at the point p by a unit source distribution over the surface element dS at the point q.

The corresponding equation for a two-dimensional problem takes the closely related form

$$\sigma(p) - \int_C \sigma(q)K(p,q)ds = -\vec{n}(p) \cdot \vec{V}_\infty \tag{2}$$

where the kernel function K now takes on a simpler form. However, when equations (1) and (2) are discretized, both lead to a matrix equation of the form

$$\sigma_i - \sum_{j=1}^{m} A_{ij}\sigma_j = f_i \qquad i = 1, \ldots m \tag{3}$$

where m is the total number of surface panels or arc length elements. The values A_{ij} are known as the influence coefficient matrix. Thus, it can be seen that, in principle, the two- and three-dimensional problems are mathematically equivalent, although in general the value of m will be much larger and the calculation of the influence coefficients will be more complicated for three-dimensional flows. Also, the structure of the matrix $[A_{ij}]$ and the

column vectors $[\sigma_j]$ and $[f_i]$ will be rather different in the two cases. This point will, however, be considered in greater detail in section 6 when the extension of the mode-function concept to three-dimensional problems is discussed. The theory and results presented here will therefore be directed at the two-dimensional problem.

The standard solution method based on a source distribution combines the "self-influence term" with the remaining terms to recast equation (3) as

$$\sum_{j=1}^{m} A'_{ij}\sigma_j = f_i \qquad i = 1, \ldots m \tag{4}$$

where $A'_{ij} = \delta_{ij} - A_{ij}$. This equation now takes on a form more closely related to an integral equation of the first kind. However, since $A_{ij} << 1$, it should be noted that it still possesses the essential qualities associated with integral equations of the second kind, namely that the matrix $[A'_{ij}]$ is diagonally dominant. Therefore, it has desirable characteristics for solution both by direct Gaussian elimination and by iterative methods. It will be shown in section 4.5 that this property is also necessary for the success of the mode-function method presented here.

From the mode-function point of view, the matrix A'_{ij}, regarded as discrete values of a function of two variables, has the undesirable property that it has a large spike corresponding to the dominant diagonal. Since we seek to fit the matrix in terms of smoothly varying mode functions, it is therefore natural to treat the formulation given in (3) and attempt to fit the matrix A_{ij}.

2.0 GENERAL THEORY

2.1 The Eigenvector Form

Having established the background for the mode-function concept, it is now appropriate to present the theory and establish a notation for a more detailed discussion. The eigenvector method will be presented first since this can provide some insight into the question of whether to use a formulation based on equations of the first or the second kind. Despite the close relationship between such equations, it should be pointed out that this is not simply a question of whether or not the diagonal term is included in the matrix. If a normal-velocity boundary condition is used, a pure source distribution leads to an equation which has the natural form of an equation of the second kind, whereas a pure vortex distribution will lead to an equation of the first kind.

Matrix notation will be used throughout since some of the more involved aspects of the Fourier version to be presented in subsequent sections can most easily be condensed into such a format. Thus, equations (3) or (4) can be represented as

$$\underline{f} = \underline{\rho} - A\underline{\rho} = A'\underline{\rho} \tag{5}$$

where $\underline{f}$ and $\underline{\rho}$ are column vectors consisting of the given "onset flow" and the unknown singularity distribution while A and A' are the two different forms for the influence coefficient matrix. The precise form of these matrices will depend both on the type of singularity distribution selected and on the way in which the problem is discretized. However, to simplify the discussion, it will be expedient to introduce the base case in which $\underline{\rho}$ is the source density, assumed to be constant over each element, and A is obtained by integrating the kernel over linear elements. The modifications introduced by the application of the mode-function method to alternative singularity distributions, presented in section 5, is straightforward.

Pursuing first the idea of fitting the matrix A in equation (5), note that it can be regarded as a function of two variables defined at m^2 equally spaced intervals, where the independent variables correspond to the row and column numbers. By separation of variables, this function can be approximated by a

product of two functions $\underline{f} = (f_1, f_2, \ldots f_m)$ and $\underline{g} = (g_1, g_2, \ldots g_m)$ dependent on the row and column number, respectively. Thus, an element A_{ij} of the A matrix is approximated by $f_i g_j$ and the square of the error invclved in this approximation is

$$\sum_{j=1}^{m}\sum_{i=1}^{m} (A_{ij} - f_i g_j)^2 \tag{6}$$

Differentiating this expression with respect to f_i and g_j leads to the conditions under which this error will be a minimum. Thus

$$A\underline{g} = k^2\underline{f}, \qquad k^2 = g_1^2 + g_2^2 + \ldots + g_m^2$$

and (7)

$$\tilde{A}\underline{f} = h^2\underline{g}, \qquad h^2 = f_1^2 + f_2^2 + \ldots + f_m^2$$

where $\tilde{A}$ is the transpose of A. Therefore, $\underline{f}$ and $\underline{g}$ will be eigenvectors of the matrices $A\tilde{A}$ and $\tilde{A}A$ since

$$A\tilde{A}\underline{f} = h^2k^2\underline{f}$$

and (8)

$$\tilde{A}A\underline{g} = h^2k^2\underline{g}$$

Now $A\tilde{A}$ and $\tilde{A}A$ are symmetric matrices and so, provided that their eigenvalues are distinct, they will each possess a set of orthogonal eigenvectors which must satisfy

$$A\underline{g}_k = \lambda_k\underline{f}_k$$

and (9)

$$\tilde{A}\underline{f}_k = \lambda_k\underline{g}_k$$

or

$$A\tilde{A}\underline{f}_k = \lambda_k^2\underline{f}_k$$

and

$$\tilde{A}A\underline{g}_k = \lambda_k^2\underline{g}_k , \qquad k = 1, 2, \ldots m \tag{10}$$

The corresponding fit in terms of the first n of these eigenvectors is

$$A = \lambda_1\underline{f}_1\tilde{\underline{g}}_1 + \lambda_2\underline{f}_2\tilde{\underline{g}}_2 + \ldots + \lambda_n\underline{f}_n\tilde{\underline{g}}_n \tag{11}$$

There are several points about this scheme which should be made at this stage. The procedure would be out of the question if the eigenvectors had to be calculated directly from equation (10) since the formation of the matrix products $A\tilde{A}$ and $\tilde{A}A$ would require $0(m^3)$ operations, and so this operation alone would require more computer time than the direct solution. However, it is possible to show that an adaptation of the traditional power method of iteration can be applied to equation (9), and one eigenvector can be calculated in $0(pm^2)$ operations where p is the number of iterations required (typically $p \sim 5$ or 6). It is therefore clear that, in order for this method to be competitive with the direct matrix solution, n must be small compared with m since the operation count could otherwise approach or exceed $0(m^3/3)$ which is required for the direct solution.

In terms of the matrix notation, equation (11) can be written

$$A = FD\tilde{G} \tag{12}$$

where D is the diagonal $(n \times n)$ matrix of eigenvalues and F and G are the basic $(m \times n)$ "fit matrices" whose columns are defined by the eigenvectors $\underline{f}_k$ and $\underline{g}_k$ $(k = 1, \ldots n)$, respectively. Similarly, one can express the vectors $\underline{f}$ and $\underline{\rho}$ in terms of the matrix G to give

$$\underline{f} = G\underline{b} \qquad \text{and} \qquad \underline{\rho} = G\underline{a} \tag{13}$$

so that equation (5) can be written

$$G\underline{b} = G\underline{a} - FD\tilde{G}G\underline{a} \tag{14}$$

It has been noted that the eigenvectors $\underline{f}_k$ and $\underline{g}_k$ form two orthogonal sets of vectors and so, choosing them to have unit length, it follows that the matrix G is orthogonal, so that $\tilde{G}G = I$. Equation (14), therefore, gives

$$\underline{b} = \underline{a} - C\underline{a} \qquad \text{where} \qquad C = \tilde{G}FD \tag{15}$$

The solution of this equation will involve $0(n^3/3)$ operations, but we have already asserted that the scheme will only be competitive if an adequate approximation to equation (5) can be obtained for $n << m$. Thus, the solution time for equation (15) will be negligible compared with the time required to find the eigenvectors.

The accuracy of this truncated equation will in turn be governed by the fittability of the matrix A and the nature of the vectors $\underline{f}$ and $\underline{\rho}$. Since the

behavior of these eigenvector expansions is unknown a priori, the validity of this truncation must be based primarily on the numerical results obtained. This situation contrasts strongly with Fourier series where the behavior and the factors governing convergence are well understood.

Before proceeding with an outline of the theory behind the Fourier series expansion, it will be worthwhile to derive the truncated eigenvector equation corresponding to an integral equation of the first kind since this throws some light on the general fittability of such equations. If F' and G' are the eigenvector matrices corresponding to the matrix A' then, following equations (12) and (13)

$$A' = F'D'\tilde{G}'$$

and

$$\underline{f} = F'\underline{d}' \qquad \text{and} \qquad \underline{\rho} = G'\underline{a}' \tag{16}$$

Equation (5) can then be written as

$$\underline{d}' = D'\underline{a}'$$

or

$$a_k' = d_k'/\lambda_k' \qquad k = 1, \ldots n \tag{17}$$

It follows that, since the eigenvalues λ_k' decrease as k increases, the expansion for $\underline{\rho}$ will only converge if the numbers d_k' decrease even more rapidly. The form of equation (17) does indicate, however, that for problems which fall naturally into the form of an equation of the first kind, the convergence of the eigenvector expansion of the solution will be poor. This is consistent with the results derived from the Fourier expansion method for which unsatisfactory results were obtained when applied to an equation in this form. In fact, the method presented in section 4.5 is shown to be valid only for equations of the second kind for which the corresponding matrix A' possesses a dominant diagonal.

2.2 The Fourier Form

Much of the discussion given in the previous section is also applicable to the Fourier format, and so the theory can be presented more briefly. It should be noted at the outset that this mode of fitting relies on the existence of known rapid calculation methods and known artifices to accelerate convergence

even though Fourier series as such have no particular relationship to Neumann kernel functions. It is, however, based on the observation that the right-hand side vector $\underline{f}$, the source vector $\underline{\rho}$ and the influence matrix are arrays of numerical values which are necessarily periodic since $f_1 = f_{m+1}$, $\rho_1 = \rho_{m+1}$, $A_{i,1} = A_{i,m+1}$ and $A_{1,j} = A_{m+1,j}$. For instance, in figure 2, with $m = 12$ the points $i = 1$ and $i = 13$ will be identical. The analysis presented in this section will be based on this periodic behavior although it should be noted that in practice there may arise discontinuities in the fitted vectors such as that occurring across the sharp trailing edge of an airfoil. Modifications to the fitting procedure necessary to cope with such discontinuities will be presented in section 4.

The best rate of convergence for a finite Fourier series is obtained by using a pure sine series. However, such a series will vanish at the ends of the interval over which the series is defined, and so to fit a general function an additional constant must be introduced. Thus, if the function to be fitted is defined by the values $(f_1, f_2, \ldots f_m)$ the series expansion will be

$$f_j = b_1 + \sum_{k=2}^{m} b_k \sin(j-1)(k-1)h \qquad \text{where} \qquad h = \pi/m \tag{18}$$

In this expression, $b_1 = f_1$ and the remaining coefficients are the standard Fourier sine coefficients of the function values $(f_j - b_1)$. Using the matrix notation introduced in the previous section, this can be written

$$\underline{f} = G\underline{b} \tag{19}$$

in which the transformation matrix now has the form

$$G = \begin{bmatrix} 1 & 0 & 0 & \cdot & \cdot & \cdot & 0 \\ 1 & S_{11} & S_{12} & \cdot & \cdot & \cdot & S_{1,m-1} \\ 1 & S_{21} & S_{22} & \cdot & \cdot & \cdot & S_{2,m-1} \\ \cdot & \cdot & \cdot & \cdot & \cdot & \cdot & \cdot \\ \cdot & \cdot & \cdot & \cdot & \cdot & \cdot & \cdot \\ \cdot & \cdot & \cdot & \cdot & \cdot & \cdot & \cdot \\ 1 & S_{m-1,1} & S_{m-1,2} & \cdot & \cdot & \cdot & S_{m-1,m-1} \end{bmatrix} \tag{20}$$

where $S_{ij} = \sin(ijh)$, $h = \pi/m$. Similarly, the source density can be expressed as a sine expansion with coefficients $\underline{a}$,

$$\underline{\rho} = G\underline{a} \tag{21}$$

Application of this process first to the rows of A and then to the columns of the resulting matrix leads to

$$A = GB\tilde{G} \tag{22}$$

where B is a matrix consisting primarily of Fourier coefficients.

The elements of $\underline{b}$ and B can be obtained by the application of the FFT algorithm to one- or two-dimensional arrays. Substitution of these expressions into equation (5) gives

$$G\underline{b} = G\underline{a} - GB\tilde{G}G\underline{a} \tag{23}$$

Let $D = \tilde{G}G$, then D can be shown to have the form

$$D = \begin{bmatrix} m & \sigma_1 & \sigma_2 & \cdots & \sigma_{m-1} \\ \sigma_1 & m/2 & & & \\ \sigma_2 & & m/2 & & \\ \vdots & & & \ddots & \\ \sigma_{m-1} & & & & m/2 \end{bmatrix} \tag{24}$$

where

$$\sigma_k = \cot(kh/2) \qquad (k \text{ odd})$$
$$= 0 \qquad (k \text{ even})$$

The simple structure of the matrix D will make the calculation of the product BD very rapid.

Since the matrix G is nonsingular, equation (23) can therefore be written as

$$\underline{b} = \underline{a} - C\underline{a} \qquad \text{where} \qquad C = BD \tag{25}$$

This represents a set of m equations in m unknowns which is exactly equivalent to the original system of equations. However, if we assume that the known vector $\underline{f}$ and the solution vector $\underline{\rho}$ can be adequately represented in terms of their first n coefficients, then equation (25) can be truncated to give a system of n equations in n unknowns. The precise conditions under which this truncation are valid are discussed in detail in section 4.5 at which time an improved scheme is developed. However, since this simple truncation is used for most of the results presented, further discussion of this point can be postponed until section 4.5.

3.0 APPLICATION OF THEORY TO SMOOTH AIRFOILS

3.1 Definition of Test Case Airfoils

For the initial testing of the mode-function method, several special airfoils were used in order to give direct control of such factors as: (a) smoothness, (b) accuracy of surface definition, (c) exactness of velocity distribution, etc. These airfoils were defined by the "pole" theory of James (ref. 5) which uses conformal mapping from a unit circle. The two smooth airfoils used are designated E33 and E13 and their shapes are shown in figures 3 and 4.

The E33 airfoil has a high curvature in the trailing-edge region but no actual discontinuity in surface slope. The source density as a function of the arc length will be continuous but there is a sharp peak around the trailing-edge region and so the airfoil does provide a severe test case. The second airfoil, E13, does not possess the high curvature of E33 and so it provides a much simpler test case. However, comparison of the results for these two airfoils provides a useful guide as to how this high curvature affects the rate of convergence of the solution for the different methods being tested. It should be noted that, for all the results presented here, the point numbering starts from the trailing edge or rear stagnation point and proceeds in a counterclockwise direction around the leading edge and back to the starting point. (See fig. 2).

Before presenting the results obtained for these two airfoils it will be worthwhile to consider the question of the fittability of the normal velocity matrix. As previously noted in section 1.3, the matrix A' in equation (5) is not well suited to fitting since it possesses a large spike on the diagonal, but the matrix A has a smoother behavior. The 49th row of a 96-element matrix A, corresponding to the negative of the normal velocity induced at the 49th control point by the other elements (see fig. 3), is shown in figure 5. The Neumann matrix used here is based on linear elements with constant source strength on each element and so the diagonal term in A is zero giving rise to the spike shown at $j = 49$ in figure 5. This could be removed by including a term dependent on the airfoil curvature as in the higher-order method (ref. 6). However, numerical results indicate that this effect is of little importance, and it is clearly small compared with that found in the A' matrix where the value jumps from about 0.05

to 1.0. Therefore, the source distribution results presented here are all based on the lower-order matrix formulation. Of greater significance as far as the fittability is concerned is the secondary spike caused by the influence of the source elements at control points on the opposite surface of the airfoil. This can be particularly severe for a thin airfoil where the control point on one surface can approach very close to the source elements on the opposite surface. Figure 6 illustrates this effect, showing the behavior of the 21st row of the matrix A (see fig. 3) for the E33 airfoil. There is no way of removing this contribution prior to fitting, and so this effect can be expected to govern the number of terms required to obtain an accurate solution. The use of alternative singularity mixes might be expected to alleviate this problem since a vorticity distribution is known to behave well for thin airfoils. This topic will, however, be discussed in greater detail in section 5.

3.2 Eigenvector Series Results

It was pointed out in section 2.1 that the number of operations required to calculate n eigenvectors associated with a matrix of order m is $0(p\ n\ m^2)$ where p, the number of iterations required, is about 5 or 6. Therefore, to be competitive with a direct solution, the eigenvector method must give acceptable answers for $n \sim m/(3p) \sim m/15$ and to give an improvement in the computer time, a significantly smaller value for n would be required.

Results obtained for airfoil E33 with 96 points, presented in figures 7-9, indicate that this efficiency requirement cannot be achieved. These results show the source density and the tangential velocity distribution, plotted against the normalized arc length. Thus, for $n = 20$ or $n/m \sim 1/5$, the source density and the velocity distribution in figures 7 and 8 are inadequate. For $n = 30$ the velocity distribution, figure 9, still possesses a significant oscillation. The results for the 96-point E13 airfoil are even more unsatisfactory with the source density, shown in figures 10 and 11, still oscillating badly even for $n = 40$, or $n/m \sim 2/5$.

On the basis of these results, the basic eigenvector method does not offer any advantage over the direct matrix solution and, unlike the Fourier expansion method, there is no way in which the method can be improved, given the present

state of the art. In addition, there does not appear to be any reason why the results for three-dimensional problems should be any more favorable. In the light of these results, further work has been concentrated on the Fourier method outlined in section 2.2 which does appear to offer significant improvements in computation times. The results obtained with the basic Fourier method will be shown to be much more encouraging, and in addition, there are various techniques which can be applied to improve the convergence and which are not available for the eigenvector method. In particular, the use of the FFT algorithm enables all of the Fourier coefficients for the matrix to be calculated in $O(2S_m m^2)$ operations where S_m is the sum of all of the prime factors of m, and this knowledge of all the coefficients is crucial to the improved truncation scheme to be presented in section 4.5.

3.3 Sine Series Results

A good starting point for the sine fit results is the E13 airfoil for which the eigenvector series results, figures 10 and 11, were so poor. Thus, figure 12 shows the 24-term sine series fit to the source density for this airfoil from which it is clear that superior results are obtained for a smaller number of terms. A similar encouraging trend is observed for the E33 airfoil; figure 13 shows the source distribution, plotted against the arc length around the airfoil, obtained with a 24-term sine series. Also shown in this figure is the same solution after the application of σ-smoothing to the expansion coefficients. This technique applies an attenuation factor to the Fourier coefficients such that the influence of the higher harmonics is decreased. The overall error is increased, but it can be seen that the residual oscillation is reduced leading to a more acceptable solution. The corresponding tangential velocity distribution for the 24-term expansion (without σ-smoothing) is shown in figure 14. This truncated solution reproduces the sharp peak around the trailing edge remarkably well although there is a significant oscillation present in the distribution. The amplitude of the oscillation is considerably reduced by including 32 terms as in figure 15. Alternatively, the oscillation could be reduced by the application of σ-smoothing, although this would reduce the overall agreement. These results, therefore, illustrate the potential of the basic sine fitting procedure although the crucial test for the technique must be based on realistic airfoil shapes with sharp trailing edges.

4.0 APPLICATION TO AIRFOILS WITH SHARP TRAILING EDGES

4.1 The Basic Sine Series Fit

As mentioned in the previous section, the combination of the long computation times and the poor convergence makes the eigenvector series fit an uneconomic proposition. This section will therefore present results obtained by the application of the sine series fit of section 2.2 to airfoils with sharp trailing edges. Sections 4.2 to 4.4 will describe some modifications to the basic fitting procedure introduced to improve the convergence, and section 4.5 will introduce a new matrix truncation scheme which enables an approximate solution to be obtained for all of the expansion coefficients of the source density.

The first sharp airfoil considered is designated BCC#2 and is shown in figure 16. This is a very thick airfoil and so it provides a straightforward test case with which to continue the validation of the mode-function concept. With the freestream parallel to the arrow in figure 16, this airfoil generates no lift and at this incidence excellent results were obtained with the basic sine series method. The velocity distribution for $m = 96$ with 8, 12 and 16 terms is shown in figures 17-19. A reasonable approximation is obtained with only 8 terms and for 16 terms the truncated solution is almost identical to the full solution.

However, when the airfoil is rotated through about 10°, the results from this basic method became unsatisfactory. A sharp oscillation in the velocity distribution develops near the trailing edge, and this is present even when as many as 40 terms are used. An examination of the way in which the Kutta condition is satisfied for a lifting airfoil reveals the cause of this failure. The singularity distribution consists of two components, the first a pure source distribution which satisfies the boundary condition on the airfoil due to the on flow and the second a constant vortex plus a varying source distribution which together satisfy a zero normal velocity on the airfoil. These components are then combined to satisfy the Kutta condition at the trailing edge. For a lifting airfoil, each of these components becomes singular at a sharp trailing edge, but in the full Neumann solution these two singular terms cancel and the resulting source distribution is finite at the trailing edge. However, when the solution is truncated, these two singular components are inaccurately approximated and the errors are not

eliminated when the combined solution is formed. In order to overcome this problem, several modifications to the basic method have been investigated, the first two aimed at improving the fitting method in order to cope with singular functions while the third method reformulates the Kutta condition so that it is satisfied simultaneously with the remaining equations thereby ensuring that the source distribution to be fitted is finite at the trailing edge.

4.2 The Linear Fit

It will be recalled that the basic sine series fit, equation (18), assumes that the function to be fitted is periodic with $f_1 = f_{m+1}$. This is true in theory for a closed body, but if the function to be fitted contains a singularity at the trailing edge, there will be a large discontinuity between the values f_m and f_{m+1}. However, by subtracting a linear function of the point number, it is possible to ensure that the values to be fitted are zero at both ends of the interval. Therefore, to fit the vector $\underline{f} = (f_1, f_2, \ldots f_m)$ we first define the vector $\underline{g}$ by

$$g_j = f_j - \frac{m-j}{m-1} f_1 - \frac{j-1}{m-1} f_m, \qquad j = 1, 2, \ldots m \tag{26}$$

Thus $g_1 = g_m = 0$ and this vector can now be expressed as a sine series, and so equation (18) can be replaced by

$$f_j = \frac{m-j}{m-1} b_1 + \frac{j-1}{m-1} b_2 + \sum_{k=3}^{m} b_k \sin[(k-2)(j-1)h] \tag{27}$$

where $b_1 = f_1$, $b_2 = f_m$ and where h is now given by $h = \pi/(m-1)$. The transformation matrix G is therefore given by

$$G = \begin{bmatrix} 1 & 0 & 0 & \cdots & 0 \\ (m-2)/(m-1) & 1/(m-1) & S_{11} & \cdots & S_{1,m-2} \\ (m-3)/(m-1) & 2/(m-1) & S_{21} & \cdots & S_{2,m-2} \\ \cdot & \cdot & \cdot & \cdots & \cdot \\ \cdot & \cdot & \cdot & \cdots & \cdot \\ \cdot & \cdot & \cdot & \cdots & \cdot \\ 1/(m-1) & (m-2)/(m-1) & S_{m-2,1} & \cdots & S_{m-2,m-2} \\ 0 & 1 & 0 & \cdots & 0 \end{bmatrix} \tag{28}$$

where $S_{ij} = \sin(ijh)$.

This modified fitting procedure is applied both to the influence matrix and the column vectors so that the details of the application closely follow those given in section 2.2 for the basic method. The matrix product $D = \tilde{G}G$ still takes on the relatively simple structure

$$D = \begin{bmatrix} c_1 & c_2 & \sigma_1 & \sigma_2 & \cdots & \sigma_{m-2} \\ c_2 & c_1 & \sigma_1 & -\sigma_2 & \cdots & (-1)^{m-1}\sigma_{m-2} \\ \sigma_1 & \sigma_1 & (m-1)/2 & & & \\ \sigma_2 & -\sigma_2 & & (m-1)/2 & & \\ \vdots & \vdots & & & \ddots & \\ \sigma_{m-2} & (-1)^{m-1}\sigma_{m-2} & & & & (m-1)/2 \end{bmatrix} \tag{29}$$

where

$$c_1 = m(2m-1)/[6(m-1)],$$

$$c_2 = m(m-2)/[6(m-1)]$$

and

$$\sigma_i = \frac{1}{2}\cot\left(\frac{1}{2}ih\right), \qquad i = 1, 2, \ldots m-2$$

This can now be substituted into equation (25) to give a new coefficient equation which is solved in precisely the same way as in the basic method.

The results obtained for the lifting airfoil BCC#2 are encouraging with the velocity distribution obtained with $n = 24$ and $n = 32$ shown in figures 20 and 21. This represents a significant improvement over the basic method, although the oscillation present for the 24-term solution develops rapidly as n is further reduced. Comparison of equations (18) and (27) indicates that the number of Fourier coefficients has been reduced from $(m-1)$ to $(m-2)$. However, the FFT routine used places some restrictions on this quantity. Therefore, the airfoil point number has been increased by one for these and subsequent results.

4.3 The Singular Fit

The breakdown of the results presented above for small values of n indicates that the singular behavior of the source density still presents a problem for the fitting procedure. It was therefore decided to further modify the technique in order to remove the singular contribution before fitting the function. As a very crude approximation, the singular behavior of the source density can be expressed as the inverse of the point number variable. Reference to equation (26) therefore leads to the definition of the vector to be fitted $\underline{g}$ as

$$g_j = f_j - \frac{b_1}{m+1-j} - \frac{b_2}{j}, \qquad j = 1, 2, \ldots m \tag{30}$$

where b_1 and b_2 are defined in terms of f_1 and f_m such that $g_1 = g_m = 0$. Expressing $\underline{g}$ in terms of a sine series immediately gives

$$f_j = \frac{1}{m+1-j} b_1 + \frac{1}{j} b_2 + \sum_{k=3}^{m} b_k \sin[(k-2)(j-1)h] \quad \text{where} \quad h = \pi/(m-1) \tag{31}$$

Comparison of this with equation (27) shows that in the definition of the transformation matrix G, equation (28), only the first two columns will be changed. Thus

$$G = \begin{bmatrix} 1/m & 1 & 0 & . & . & . & 0 \\ 1/m\text{-}1 & 1/2 & S_{11} & . & . & . & S_{1,m-2} \\ . & . & . & . & . & . & . \\ . & . & . & . & . & . & . \\ . & . & . & . & . & . & . \\ 1 & 1/m & 0 & . & . & . & 0 \end{bmatrix} \tag{32}$$

As with the linear fitting method described in the previous section, this technique is applied to each of the vectors and the influence matrix in equation (5) although it is primarily aimed at improving the fit to the source density vector.

It can now be shown that the matrix $D = \bar{G}G$ will still be given by equation (29) with

$$c_1 = \sum_{k=1}^{m} \frac{1}{k^2} ,$$

$$c_2 = \frac{2}{m+1} \sum_{k=1}^{m} \frac{1}{\kappa} \qquad (33)$$

and

$$\sigma_i = \sum_{k=1}^{m-2} \frac{1}{m-k} \sin\left(\frac{ik\pi}{m-1}\right) , \quad i = 1, 2, \ldots m-2$$

The application of this method therefore follows very closely that of the linear fitting method once the definition of these constants has been changed.

This method was applied to the lifting airfoil, BCC#2, defined by 49 points and the results are shown in figures 22 and 23 for $n = 16$ and $n = 20$. This reduction in point number provides a more realistic value for m, but it does not lead to a proportionate reduction in n for a given quality solution. The results, therefore, provide a more realistic estimate of the ratio n/m. It can be seen that, even for this very crude approximation to the singular behavior of the source density, a significant improvement in the truncated solution is achieved. A reasonable agreement in the velocity distribution is achieved for $n = 16$ and for $n = 20$ the results are very close to the full solution except near the trailing edge.

4.4 The Combined Kutta Condition

The results of the previous two sections illustrate that the basic sine fitting procedure can be adapted to cope with the singular source distribution which occurs in the calculation of the flow over a lifting airfoil. However, figure 23 still shows a discrepancy between the truncated solution and the full solution near the trailing edge. This could be significant if the results were required for a boundary-layer calculation and so the precise form of the singularity to be removed prior to fitting would need to be investigated further if this method were to be pursued. On the other hand, this section considers the possibility of reformulating the problem so that the calculated source density is well behaved. It was seen in section 4.1 that the basic sine fit gave excellent results for

a nonlifting airfoil for which the basic source distribution automatically satisfies the Kutta condition. Therefore, if the circulation is treated as an additional unknown, the Kutta condition can be satisfied simultaneously with the source strength equations and the resulting source distribution will be finite at the trailing edge.

This will now give a system of $m + 1$ equations in $m + 1$ unknowns which could, in principle, be solved by the direct application of any of the fitting procedures described above. However, this is not practical since the additional values added to the matrix and the column vectors will destroy their continuous nature upon which this method relies. For instance, a new column vector would be defined consisting of the source strengths and the circulation. Since the circulation will not be directly related to the adjacent source values, there will be a discontinuity in this modified vector. Such discontinuities cannot be adequately represented by continuous functions and so the total circulation will be poorly approximated, and the resulting solution will be slowly convergent in n.

It is, however, possible to eliminate the circulation numerically and then apply the fitting technique to the modified $m \times m$ matrix. This approach has been applied to the lifting BCC#2 airfoil and the results are shown in figures 24 and 25 for $n = 12$ and $n = 16$. The linear fitting described in section 4.2 and σ-smoothing were used and the resulting velocity distribution is very well behaved. Although the agreement near the leading edge is worse than that shown in figures 22 and 23, the undesirable oscillation near the trailing edge has been removed.

4.5 An Improved Matrix Truncation Scheme

While the results presented so far are encouraging, it should be pointed out that these results are all based on the BCC#2 airfoil which, as noted earlier, is a very thick airfoil. The next step is therefore to test the method on an airfoil with a more realistic thickness, and that used is shown in figure 26. This is simply a scaled version of BCC#2, having been derived by dividing the y-ordinate of the thick airfoil by 3 and rotating the resulting points through 5°. As the thickness of the airfoil is reduced, the peak in the influence matrix resulting from the effect of the source elements on the opposite surface, illustrated in figure 6, becomes more pronounced. Therefore, this airfoil provides a more severe

test case since the fittability of the matrix is impaired. The effect of this can be seen in figures 27 and 28 which show the velocity distribution for this airfoil using the method of section 4.4 with $n = 16$ and $n = 20$, respectively.

It is clear that even with 20 terms, or $n/m \sim 2/5$, the results of the truncated solution are inadequate, while the use of a greater number of terms would detract from the computational efficiency of the mode-function method. With the use of the FFT algorithm, all of the expansion coefficients for the transformed matrix equation (25) are known but the size of the matrix equation to be solved must be kept as small as possible in order to reduce the computation time. It was, therefore, decided to examine the truncation of the matrix equation with the aim of using all of the available information to obtain an improved solution while explicitly solving only a small fraction of the equations.

The transformed coefficient equations to be solved are given by equation (25), i.e.

$$\underline{b} = \underline{a} - BD\underline{a} \tag{34}$$

where D is given either by equation (24) for the basic fit, or by equation (29) for the modified fit of sections (4.2) or (4.3). In either case the matrix B will consist primarily of Fourier coefficients. Provided that the matrix A is sufficiently smooth, the coefficients of the higher harmonics will be small compared with those of the lower harmonics. Thus, in general, the most significant information contained by the matrix B will be concentrated into the first few rows of the first few columns, i.e. the magnitude of the entries of B will decrease, in general, as the row or column number increases. Consideration of the structure of the matrix D leads to the conclusion that the matrix product $C = BD$ will have the property that, in general, its elements will decrease in magnitude as the row number increases.

In order to express these ideas in mathematical terms, the matrix C and the column vectors $\underline{a}$ and $\underline{b}$ in equation (34) can be partitioned to separate the first n rows and columns where $n < m$. Thus

$$C = \begin{bmatrix} C_{11} & C_{12} \\ C_{21} & C_{22} \end{bmatrix}$$

$$\underline{a} = \begin{bmatrix} \underline{a}_1 \\ \\ \underline{a}_2 \end{bmatrix} \qquad \text{and} \qquad \underline{b} = \begin{bmatrix} \underline{b}_1 \\ \\ \underline{b}_2 \end{bmatrix} \tag{35}$$

where C_{11} is an $n \times n$ matrix, while $\underline{a}_1$ and $\underline{b}_1$ each have n entries. From the preceeding discussion we can assert that, provided n is suitably chosen, the largest element in the $(m-n) \times n$ matrix C_{21} will be small compared with the largest element in C_{11}. Similarly the largest element in the $(m-n) \times (m-n)$ matrix C_{22} will also be small.

Substitution of equations (35) into equation (34) leads to the two simultaneous matrix equations

$$\begin{aligned} (I - C_{11})\underline{a}_1 - C_{12}\underline{a}_2 &= \underline{b}_1 \\ -C_{21}\underline{a}_1 + (I - C_{22})\underline{a}_2 &= \underline{b}_2 \end{aligned} \tag{36}$$

where the symbol I has been used to represent the $n \times n$ unit matrix in the first equation and the $(m-n) \times (m-n)$ unit matrix in the second equation. Now if n is "sufficiently large" and $\underline{b}$ and C "sufficiently smooth", then $\underline{b}_2$ and C_{21} can be neglected and these two equations can be approximated by

$$\begin{aligned} (I - C_{11})\underline{a}_1 &= \underline{b}_1 \\ \underline{a}_2 &= 0 \end{aligned} \tag{37}$$

which is the truncated form of the equation which has been used for all the results presented so far. At this stage the significance of the dominant diagonal becomes clear. If the unit matrices were absent from equation (36) then the terms C_{21}, C_{22} and $\underline{b}_2$ would all have the same order of magnitude, and the approximation $\underline{a}_2 = 0$ does not necessarily follow.

Equation (36) is exactly equivalent to the original matrix equation, but since C_{22} is small, it follows that we can make the approximation

$$(I - C_{22})^{-1} = I + C_{22} + \ldots \tag{38}$$

and so $\underline{a}_2$ can be eliminated to give

$$[I - C_{12}(I + C_{22})C_{21}(I - C_{11})^{-1}](I - C_{11})\underline{a}_1 = \underline{b}_1 + C_{12}(I + C_{22})\underline{b}_2 \qquad (39)$$

Again, since the matrix C_{21} is also small, we can introduce the second approximation

$$[I - C_{12}(I + C_{22})C_{21}(I - C_{11})^{-1}]^{-1} = I + C_{12}(I + C_{22})C_{21}(I - C_{11})^{-1} + \ldots \qquad (40)$$

Therefore, equations (36) can be approximated by

$$(I - C_{11})\underline{a}_1 = [I + C_{12}(I + C_{22})C_{21}(I - C_{11})^{-1}][\underline{b}_1 + C_{12}(I + C_{22})\underline{b}_2]$$

and

$$\underline{a}_2 = (I + C_{22})(\underline{b}_2 + C_{21}\underline{a}_1) \qquad (41)$$

The explicit calculation of any of the matrix products involved in the right-hand side of equation (41) is out of the question. However, the terms on the right-hand side can each be calculated by performing a succession of products between matrices and column vectors, together with one matrix inversion required to find $(I - C_{11})^{-1}$. It can be shown therefore that a full solution to equation (41) requires $0(n^3/3)$ operations to factorize the matrix $(I - C_{11})$ together with $0(3m^2)$ operations required to perform all of the products necessary to solve for $\underline{a}_1$ and $\underline{a}_2$. The operation count for the solution of the basic truncated equation (37) is $0(n^3/3)$, so that for an additional $0(3m^2)$ operations, the solution of (41) gives an approximation to all of the expansion coefficients. In addition, the solution for the first n coefficients $\underline{a}_1$ will also be improved since it takes into account more of the available information.

This scheme has been tested for the thin lifting airfoil, figure 26, and excellent results have been obtained. Figures 29 - 31 show the velocity distribution obtained using $n = 8$, 12, and 16, respectively, together with the linear fit of section 4.2. Thus, even for $n = 8$, this scheme can produce results which could be adequate for many applications, and for $n = 16$, or $n/m \sim 1/3$ the results are very close to the full solution.

These results serve to demonstrate the potential for this particular formulation of the mode-function method, although it should be pointed out that they do not necessarily represent the optimum. For instance, the only two approximations

used are given by equations (38) and (40). However, either of these could be made more accurate by the inclusion of higher-order terms, at the expense of increasing the number of matrix and vector products which must be calculated. A careful balance must be maintained between the need to further reduce the ratio of n/m and the additional number of operations incurred in doing so. In addition, the results in figures 29 - 31 are based on the linear fitting technique. The results of sections 4.3 and 4.4 would indicate that a further improvement could be obtained by an improved handling of the singularity which occurs in the source distribution.

5.0 ALTERNATIVE SINGULARITY MIXES

5.1 Pure Vortex Formulations

The results presented in the earlier sections have all been based on the use of a source distribution with a constant strength vortex distribution introduced in order to provide the circulation about a lifting airfoil. As mentioned in section 4.5, the normal-velocity matrix associated with such a singularity distribution can be difficult to fit for a thin airfoil. However, the matrix does possess a dominant diagonal and this has been shown to be important for the success of the improved scheme proposed in section 4.5. On the other hand, the use of a pure vortex distribution with an external normal velocity condition is known to be well suited to thin airfoil problems. The associated matrix does not develop the sharp peaks associated with thin airfoils, but it no longer possesses a dominant diagonal. In fact, the values of the elements change sign rapidly across the diagonal, and their rate of change increases as the number of elements is increased.

To investigate the relative importance of each of these two factors, the basic sine series method together with a pure vortex distribution and external normal-velocity condition was applied to the smooth airfoil E33. The vorticity distribution used was linearly varying and continuous everywhere except at the rear stagnation point, where the first and last values of the vorticity were defined to be equal and opposite.

The velocity distributions derived for $m = 96$, using 32, 36 and 40 terms, are illustrated in figures 32-34. Although the solution, shown in figure 33, obtained with 36 terms is good, this agreement must be fortuitous, since the additional terms included in figure 34 lead to a deterioration of the solution. This is clearly an unsatisfactory situation, and these results should be compared with those of figures 14 and 15 which were obtained with the same basic fitting method, but using a pure source distribution. The agreement obtained with the source method is superior and the behavior of this method was also more predictable, leading to the conclusion that the pure source matrix is more suitable for the mode-function approach. In addition, it is not at all clear whether the final method described in section 4.5 could be adapted to handle matrices of this form and so further work on this particular method was discontinued.

An alternative formulation for the pure vortex distribution is provided by satisfying the boundary condition that the internal tangential velocity is zero. This can be shown to imply that the external normal velocity also vanishes, but the numerical formulation is different. In fact, for a vortex density which is constant over each element, this problem is numerically identical to the basic source formulation used in sections 3 and 4 of this report. However, the application of this boundary condition to the continuous vortex distribution provides a convenient way of testing an alternative discretization with the mode-function method. The principal difference between the influence matrix for this problem and the basic source matrix stems from the choice of the elementary singularities used in each case. That selected for the linearly varying vortex distribution is taken to be unity at a given point on the airfoil, decreasing linearly to zero at the two adjacent points. The singularity is therefore spread out over two elements, whereas for the basic source method, the source strength is assumed to be unity over the whole length of one single element. This has the effect of spreading the "self-influence" spike out over two elements in the matrix thereby making it marginally smoother and easier to fit by the mode-function method. On the other hand, this self-influence term is no longer given simply by the unit matrix and it is no longer feasible to remove it prior to fitting.

This method has been applied to the E33 airfoil and results for $n = 24$ and $n = 32$ are shown in figures 35 and 36. Comparison with figures 14 and 15 shows roughly the same level of agreement for the basic procedure. As noted above, the matrix fitted for this vortex method still contains the unfavorable diagonal peak, and so the results indicate that this adverse influence is offset by the benefits incurred by spreading the elementary singularities out over two elements. However, this particular formulation for the influence matrix renders the application of the improved truncation scheme of section 4.5 much more complicated and probably uneconomic. Therefore, this particular formulation has not been pursued any further.

It should be noted, however, that this conclusion does not rule out the use of the mode-function method together with a linearly varying singularity distribution. The problem encountered above is a result of the particular discretization selected. Thus, the higher-order method developed by Hess (ref. 6) assumes a linearly

varying source distribution, but it allows small discontinuities in the source strength from one panel to the next. In this way the elementary singularities used are based on single elements and the resulting matrix has essentially the same fittability properties as that of the basic method used in section 4.1.

5.2 Green's Identity Formulations

The pure source distribution has been shown to be superior to the pure vortex distribution as far as the mode-function approach is concerned. However, for a thin airfoil the source strength becomes large and the use of a combined source and vortex distribution is attractive. One particularly useful combination is that based on Green's identity. This leads to source and vortex densities which are equal to the normal and tangential components of the perturbation velocity and the result is a source distribution which is more mild than the pure source distribution and a vortex distribution which is more mild than the pure vortex distribution. This approach has been investigated by Bristow (refs. 7 and 8) who has considered two alternative formulations of the problem. The source density follows immediately from the known normal velocity and so the problem reduces to that of determining the corresponding vortex density. The first approach adopted by Bristow (ref. 7) is based on the normal-velocity condition while the second (ref. 8) uses an equivalent formulation in which a uniform internal perturbation potential condition is satisfied.

The suitability of both of these approaches for use with the mode-function procedure has been studied. However, the first method based on the external normal velocity condition gives rise to a matrix of the same form as that for the pure vortex method considered in section 5.1. This particular formulation was found to give unsatisfactory results for the basic fitting procedure and the improved technique of section 4.5 cannot be applied, so that it was decided not to pursue the corresponding Green's identity approach.

The second method (ref. 8) with the internal potential condition leads to a matrix which is more ammenable to the mode-function approach. The basic sine fitting procedure in conjunction with this Green's identity formulation has therefore been tested with the BCC#2 airfoil and the results obtained are shown in figures 37-40. The first two figures show the results obtained for the

nonlifting airfoil with $m = 50$ for $n = 20$ and $n = 30$, respectively, and figures 39 and 40 give the results for the lifting airfoil for $n = 30$ and $n = 40$. The nonlifting results are worse than the corresponding results obtained with the pure source distribution for which the basic fitting method was so successful.

However, it will be recalled that this basic method failed for a lifting airfoil (see section 4.1). The Green's identity results do not break down for a lifting airfoil, but the number of terms required for an accurate solution is clearly unacceptable. The problem encountered here is similar to that referred to in section 4.4 when the Kutta condition was satisfied simultaneously with the source strength equations. In that case the problem was overcome by numerically eliminating the circulation before fitting the matrix. The truncated solution shown in figure 39 has the correct overall behavior, apart from close to the trailing edge, but the level of the velocity is displaced indicating that the total circulation is badly predicted. A similar approach to that adopted in section 4.4 could presumably be expected to improve these results also.

Therefore, this particular form of the Green's identity mix is less suited to the mode-function approach than is the pure source distribution. However, the Green's identity mix together with a potential boundary condition should, in general, lead to a matrix which is diagonally dominant and this should be ammenable to solution by the mode-function method. In view of the advantages which this mix can have for thin airfoils, further work in this direction would be worthwhile.

6.0 APPLICATION TO THREE-DIMENSIONAL PROBLEMS

6.1 Basic Approach

The results presented so far are all concerned with two-dimensional applications although, as stated in section 1.3, the numerical formulation of a three-dimensional Neumann problem is closely related to the two-dimensional case. In general, a three-dimensional application will involve a larger number of panels, and in addition, the structure of the influence matrix and the singularity vector will be rather different. It is, therefore, worthwhile to examine this structure before considering a three-dimensional application of the mode-function method.

A typical three-dimensional configuration is shown in figure 1, and in order to formulate the corresponding matrix equation for the singularity strengths, a numbering system for the panels has to be selected. A natural choice is to consider successive streamwise sections so that the wing, for instance, would be composed of k strips each consisting of m panels. The corresponding source distribution vector would, therefore, consist of k blocks,each containing m values associated with the successive streamwise sections. This vector is approximately periodic in behavior since the values around one strip would be closely related to the corresponding values on an adjacent strip. In addition, there will be discontinuities in this vector associated with the jump across the trailing edge from one strip to the next. In the light of the two-dimensional results, a global fit of this function will not produce a very rapidly convergent mode-function expansion and a sectional fitting procedure appears to be preferable.

When applied to the influence matrix, the fitting procedure first fits the rows and then the columns of the resulting matrix. Provided that the matrix can be held in the core store of the computer, this process can be accomplished efficiently. However, for a three-dimensional problem, this matrix is held on disc storage and the penalties involved in accessing this matrix by rows and then by columns could be considerable. This also indicates the need to fit the matrix in smaller blocks each of which could be held in core and again the use of $m \times m$ blocks corresponding to the individual streamwise sections appears to be the natural choice.

One final argument against the use of a global fitting method concerns the FFT algorithm. The results of section 4.5 clearly demonstrate the need to obtain all of the expansion coefficients for both the matrix and the right-hand side, and this in turn implies that the FFT algorithm must be used. It has been pointed out that this method is able to derive all of the Fourier coefficients for an $m \times m$ matrix in $O(2\ S_m\ m^2)$ operations where S_m is the sum of all of the prime factors of m. Therefore, it is necessary to choose m carefully to avoid including large prime factors which could excessively increase S_m. For instance, if m itself were a prime number, then $S_m = m$ and clearly the fitting procedure would be an $O(2m^3)$ operation and this would be uneconomic compared with the direct solutions. In fact, as programmed at Douglas Aircraft Company, the FFT routine requires that the value of m (or $(m-1)$ in the case of the modified fitting procedures of section 4.2 through 4.5) must be even and a multiple of only 2, 3 or 5. If the fitting procedure is applied to two-dimensional strips for which typically $m < 100$ this limitation is not unduly restrictive. However, as the value of m is increased, the number of acceptable values becomes more sparse. For instance, there are only 14 numbers between 2000 and 3000 which would be acceptable and this would clearly be far too restrictive. This restriction could be partially relaxed by the use of a more general FFT routine but it would still be necessary to restrict the size of the maximum prime factor to avoid S_m becoming too large, and the use of a global fitting approach may still be too restrictive.

The preferred approach to be adopted for a three-dimensional problem would, therefore, be to subdivide the matrix into blocks corresponding to the sectional strips. The diagonal blocks will be very closely related to the matrices for the two-dimensional problems considered in this report while the off-diagonal blocks will define the influence of all the points within one sectional strip upon all the control points of another sectional strip. It would not be necessary for these individual blocks to have the same dimensions, the only restriction being that each of these individual dimensions must be an acceptable value for the FFT algorithm. With the unknown source density vector and the given right-hand side vector similarly subdivided, the analysis follows very closely that given for the two-dimensional method presented here. In particular, the improved scheme presented in section 4.5 could be used and so the level of agreement and the

time saving to be expected from the mode-function approach can be based on this two-dimensional study. It will therefore be worthwhile to consider in more detail the operation count for a three-dimensional problem handled in this manner.

6.2 Operation Count for a Three-Dimensional Problem

Consider the panels to be subdivided into k strips and assume for the sake of simplicity that each strip consists of m panels. It has been mentioned that the calculation of all of the Fourier coefficients B of an $m \times m$ matrix involves $O(2\ S_m\ m^2)$ operations where S_m is the sum of all of the prime factors of m. Typically, for m between 50 and 100, S_m will be between about 11 and 15. Also the number of operations required to set up the matrix product $C = BD$ of equation (25) will be $O(2m^2)$. Therefore, to find the corresponding matrices for all the blocks of the complete matrix will involve $O[2k^2(S_m + 1)m^2]$ operations. This will give all k^2m^2 coefficients for the new matrix problem, and so the method of section 4.5 can be used. Thus, following section 4.5 let the dimensions of the matrix equation to be solved explicitly be kn. Then $O(k^3n^3/3)$ operations will be required to perform the triangular decomposition of this matrix and a further $O(3k^2m^2)$ operations will be required to complete the solution of equations (41). The total number of operations required will therefore be $O[k^2(2S_m + 5)m^2 + k^3n^3/3]$ for the mode-function solution as compared with $O(k^3m^3/3)$ for a direct solution. Thus the ratio between these two quantities will be given by

$$\left(\frac{n}{m}\right)^3 + \frac{3(2S_m + 5)}{km} \tag{42}$$

Therefore, this expression gives a guide as to the reduction in computing time required to solve the simultaneous equations which could be achieved through the use of the mode-function approach.

The results of section 4.5 indicate that it is realistic to assume that $n/m = 1/3$ although in practice it may be possible to use a smaller value for this ratio. For a typical three-dimensional configuration with $k = 40$ and $m = 50$, $S_m = 12$ and the value of (42) becomes approximately 1/12. For this particular case it would therefore be reasonable to expect the mode-function solution to be about 12 times faster than the direct solution. The computing effort in this case would be roughly equally divided between the fitting of the

matrix and the solution of the resulting equations. As the number of panels is further increased, the time required for the fitting becomes a smaller proportion of the total time. For such cases it would therefore be worthwhile to improve the approximations involved in section 4.5 in order to achieve lower values for n/m. Thus for a 4000 panel case with the assumption that $n/m = 1/4$ the mode-function method would be 26 times faster than the direct solution, and an 8000 panel case would be 38 times faster. On the other hand, an iterative solution would require $O(Ik^2m^2)$ operations for one flow condition where I is the number of iterations required. For a simple configuration such methods require 10-15 iterations, although for more complicated configurations such as those involving internal flow, more iterations may be required. Thus for one flow calculation the iterative method could, at best, be 4-5 times faster than the mode-function method for the examples considered above. However, the mode-function method does possess several properties of the direct solution which are not present in the iterative method. For instance, both the calculation of flows at different angles of attack and the simulation of boundary-layer effects require at least two flow solutions. Each such solution involves a complete calculation for the iterative method whereas for both the direct and the mode-function methods the additional solutions can be computed for very little extra cost. In addition, the solution time for the iterative method is dependent on the number of iterations required. As this can vary significantly for different configurations, this method is not always predictable. However, provided that n/m is specified beforehand, the solution time for the mode-function method will be totally predictable. Thus, any apparent advantage of the iterative method could very quickly be lost in practice.

The number of operations required to calculate n eigenvectors associated with an $m \times m$ system of equations is presently $O(pnm^2)$ where p is the number of iterations required to calculate an eigenvector. Typically $p \sim 5$ or 6 and so to be competitive with the direct solution would require $n/m \sim 1/15$ and to be competitive with the sine fitting method outlined above would require $n/m \sim 1/180$. In other words, an accurate solution for the 2000 panel example would have to be obtained with just 11 eigenvectors. The results of section 3.2 indicate that this level of agreement cannot be achieved and so the eigenvector method does not provide a viable alternative to the Fourier approach unless a more efficient process for calculating the eigenvectors could be developed.

7.0 CONCLUSIONS

The mode-function concept provides a new method for obtaining approximate solutions to large systems of linear simultaneous equations. The quantities defining many such systems can be considered as discrete values of smoothly varying functions and so they can be expressed in terms of a given set of continuous mode functions. In this way the original problem can be reformulated to give a new set of equations whose solution gives the mode-function expansion coefficients for the solution to the original problem. By truncating these expansions the number of equations to be solved is reduced and an approximate solution to the original set of equations is obtained.

This report considers the application of this technique to a two-dimensional panel method calculation of the inviscid, incompressible flow about an airfoil. Two different sets of mode functions are studied, the first are eigenvectors of a matrix related to the matrix of the original equations while the second set is composed primarily of Fourier functions. An approach to the more time-consuming three-dimensional flow problems is proposed. On the basis of the two-dimensional results obtained, a substantial reduction relative to the direct solution could be achieved in the computer time required to solve the resulting equations. The main conclusions to emerge can be summarized as follows:

1. In their basic form, neither the eigenvector series nor the Fourier series approaches to the mode-function concept give adequate results. Thus in section 3.2 it was shown that, even with a large number of terms, the eigenvector method failed to give adequate agreement for the two smooth airfoils considered. In section 4.1, the basic Fourier method was shown to fail when applied to a lifting airfoil with a sharp trailing edge.

2. The computational effort involved in deriving the eigenvectors implies that this approach will be an acceptable alternative to the direct solution only if a small proportion of the eigenvectors need be calculated. There is no way in which the basic theory can be improved to produce a competitive method without further analytical work. Therefore, this approach was not pursued any further.

3. The Fourier series approach is promising since the FFT (Fast Fourier Transform) algorithm enables all of the coefficients to be calculated in a time which is small compared with a direct matrix solution. This enables modifications to be introduced to the basic Fourier method which significantly improve the convergence of the solution. Thus the results of section 4.5 show that an accurate solution for a realistic airfoil can be obtained by explicitly solving less than 1/3 of the original number of equations.

4. The method of section 4.5 is applicable only to problems whose matrix has a dominant diagonal. When applied to the solution of a Neumann problem this restriction governs the mathematical and numerical formulation which should be used. In particular, an approach based on an unknown vortex distribution with an external normal-velocity condition will lead to an integral equation of the first kind and this is unsuitable for the mode-function version presented here. However, a source distribution formulation leads to an integral equation of the second kind and that has been shown to give good results. In addition the formulation based on Green's identity together with a potential boundary condition leads to a matrix with a similar behavior and the mode-function approach will be applicable to such problems.

5. To avoid fittability problems, the matrix should also be homogeneous in the sense that all of the original equations should be of the same form. Thus if the Kutta condition or any other equation is to be solved simultaneously with the singularity equations then this should be eliminated numerically before application of the fitting procedure.

6. The application of the mode-function method directly to a large matrix associated with a three-dimensional problem could involve several numerical and computational inefficiencies. These problems could be avoided by fitting the matrix in blocks corresponding to two-dimensional sections of the configuration. This in turn implies that the results of this two-dimensional study should be particularly relevant to the three-dimensional problems at which this technique is ultimately aimed.

7. The operation count presented in Section 6.2 indicates that for a typical problem involving 2000 panels the mode-function method could be about

12 times faster than the direct solution, and for 4000 panels the method could be 26 times faster. Furthermore, this method would possess all of the advantages of the direct solution in that the solution time for the method would be predictable and additional solutions could be obtained at a very small additional cost.

8. The method, therefore, appears to offer a promising approach to the reduction of computing costs for the solution of large three-dimensional Neumann problems which are of interest in aircraft design. Alternatively the method would offer the capability of handling larger numbers of unknowns for the same computational cost. In addition, the method should be applicable to the solution of any large system of linear simultaneous equations provided only that the matrix has a dominant diagonal, and that it is otherwise smooth.

9. Further work should be undertaken both to consider the application of this method to a Green's identity formulation in two-dimensional flow and to produce a working three-dimensional method based on either the source distribution or the Green's identity method.

8.0 REFERENCES

1. Hess, J.L.: Review of Integral Equation Techniques for Solving Potential Flow Problems with Emphasis on the Surface-Source Method. Computer Methods in Applied Mechanics and Engineering, Vol. 5, No. 2, March 1975, pp. 145-196.

2. Hess, J.L.: The Problem of Three-Dimensional Lifting Potential Flow and Its Solution by Means of Surface Singularity Distribution. Computer Methods in Applied Mechanics and Engineering, Vol. 4, No. 3, November 1974, pp. 283-319.

3. Hess, J.L. and Smith, A.M.O.: Calculation of Nonlifting Potential Flow about Arbitrary Three-Dimensional Bodies. Journal of Ship Research, Vol. 8, No. 2, September 1964, pp. 22-44.

4. Halsey, N.D. and Hess, J.L.: A Geometry Package for Generation of Input Data for a Three-Dimensional Potential-Flow Program. NASA CR 2962, June 1978.

5. James, R.M.: A General Class of Exact Airfoil Solutions. Journal of Aircraft, Vol. 9, No. 8, August 1972, pp. 574-581.

6. Hess, J.L.: Higher-Order Numerical Solution of the Integral Equation for the Two-Dimensional Neumann Problem. Computer Methods in Applied Mechanics and Engineering, Vol. 2, No. 1, February 1973, pp. 1-15.

7. Bristow, D.R.: Recent Improvements in Surface Singularity Methods for the Flow Field Analysis about Two-Dimensional Airfoils. AIAA Paper 77-641, June 1977.

8. Bristow, D.R.: Improvements in Surface Singularity Analysis and Design Methods. NASA Advanced Technology Airfoil Research Conference, Langley Research Center, 7-9 March 1978 (NASA CP 2045).

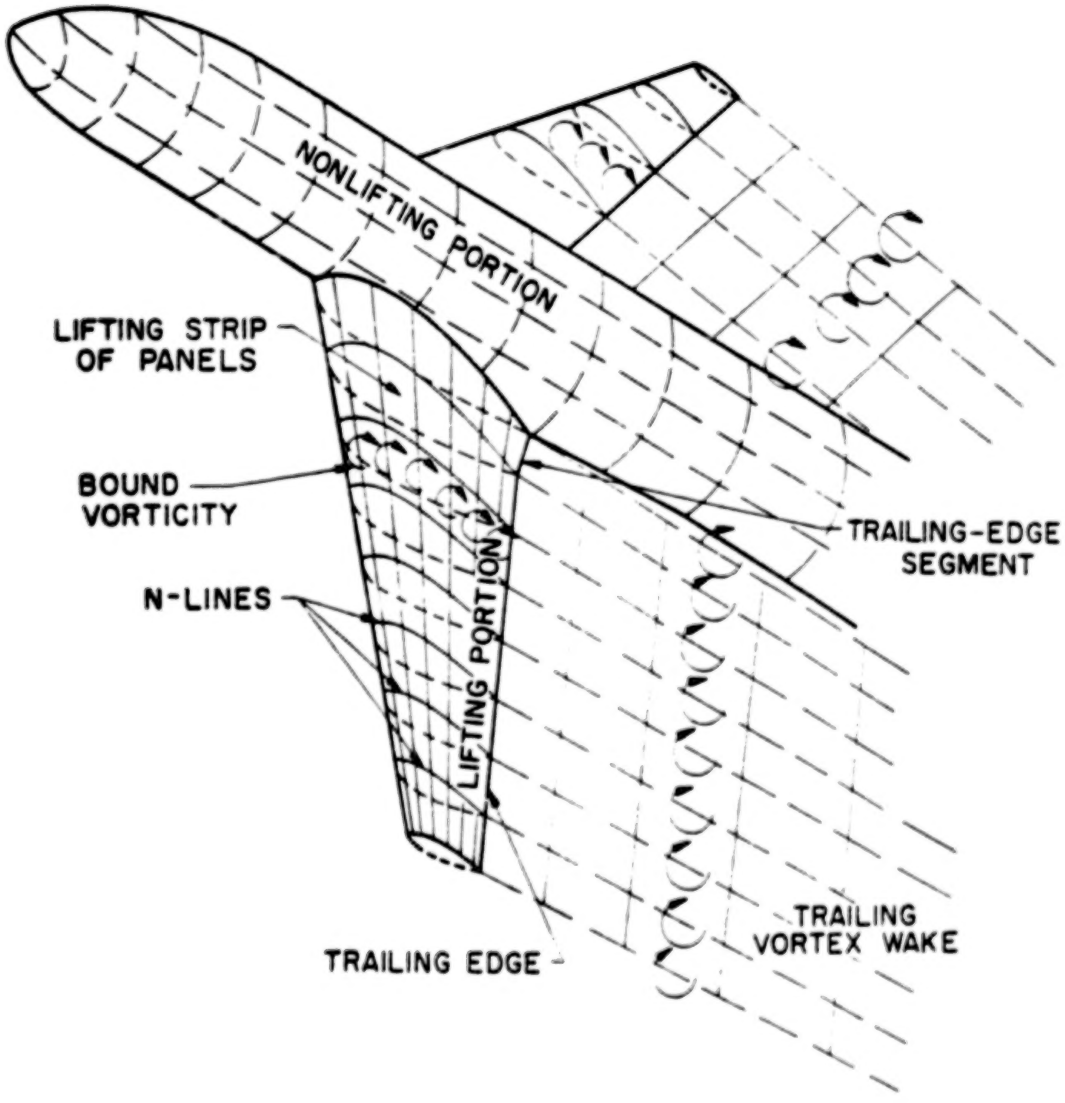

Figure 1. Representation of a three-dimensional body by surface elements.

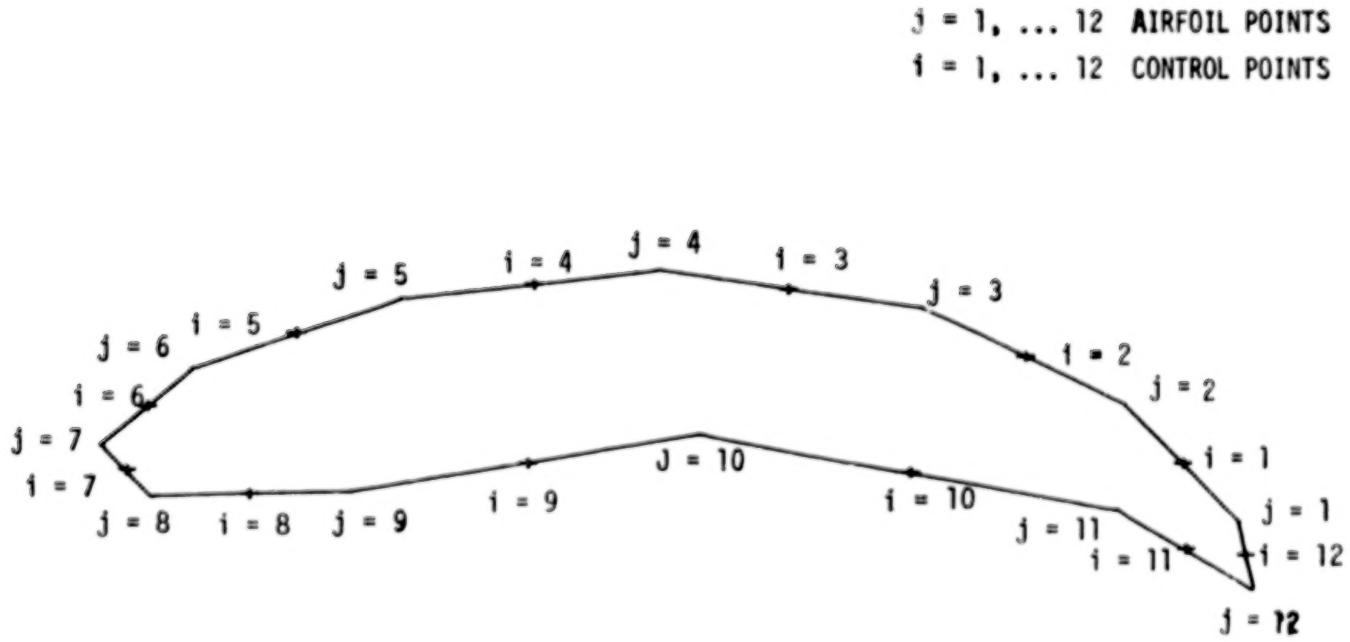

Figure 2. Linear elements and control points representing a two-dimensional body.

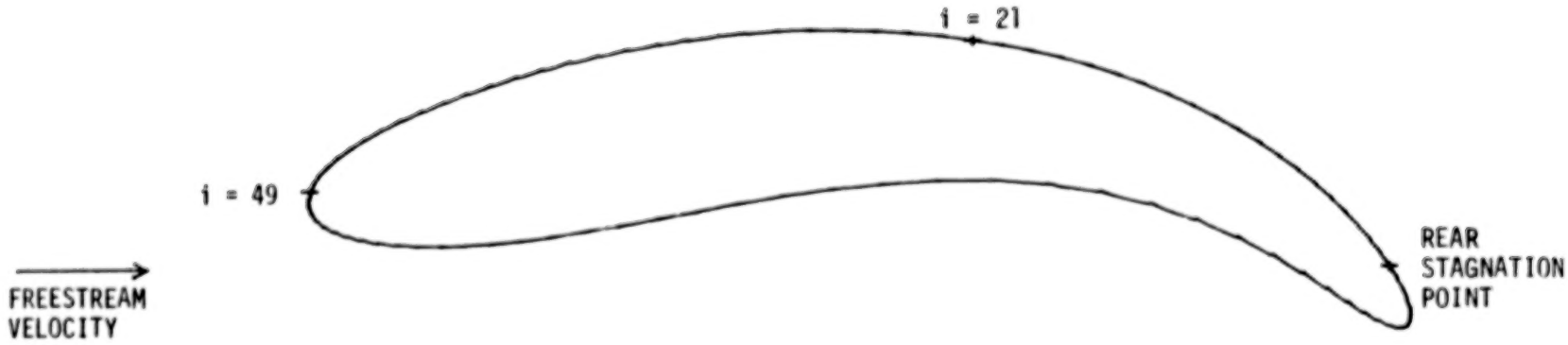

Figure 3. The E33 airfoil with a 96-element definition.

Figure 4. The E13 airfoil

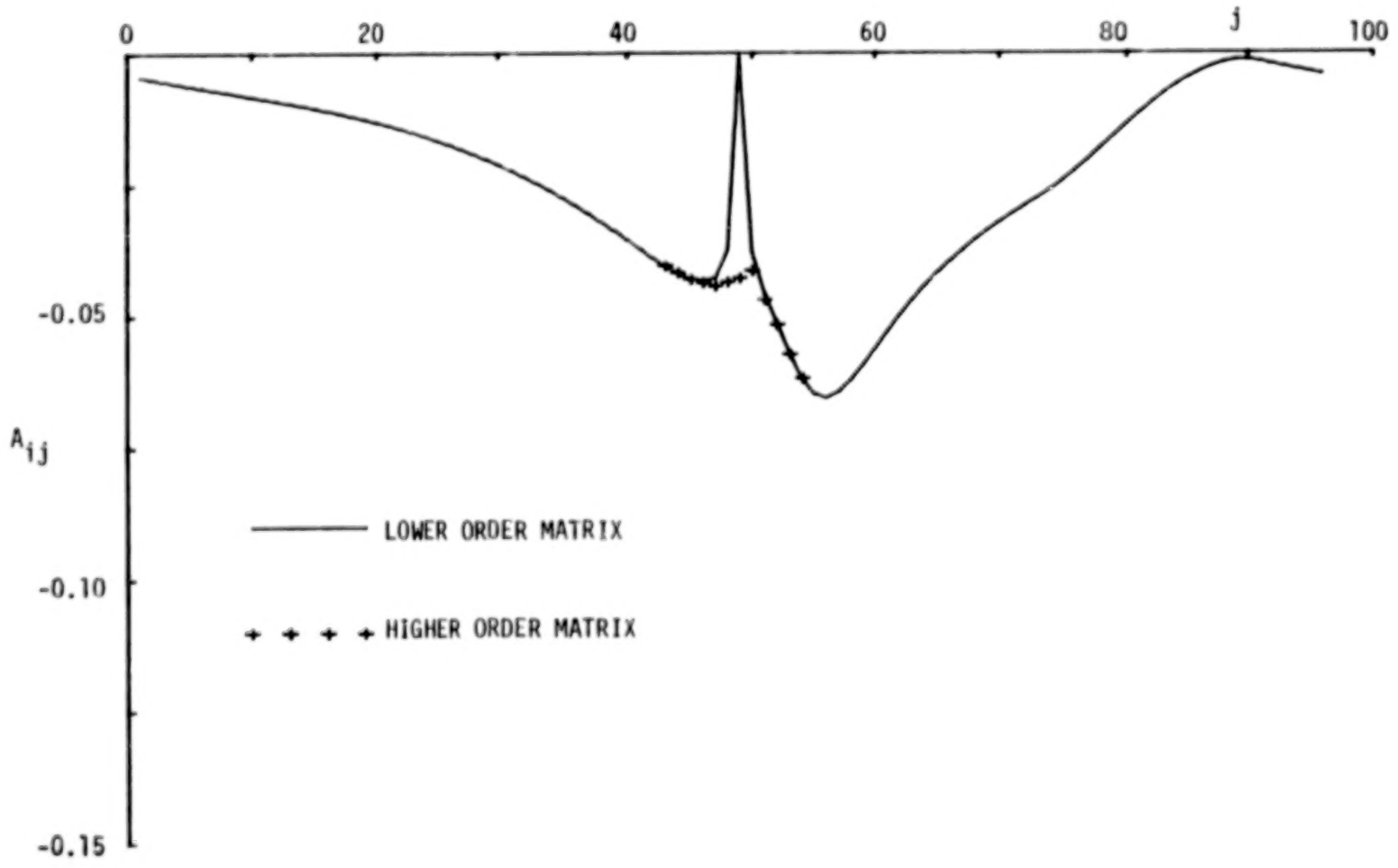

Figure 5. The behavior of A_{ij} matrix for i = 49 on the 96-point E33 airfoil.

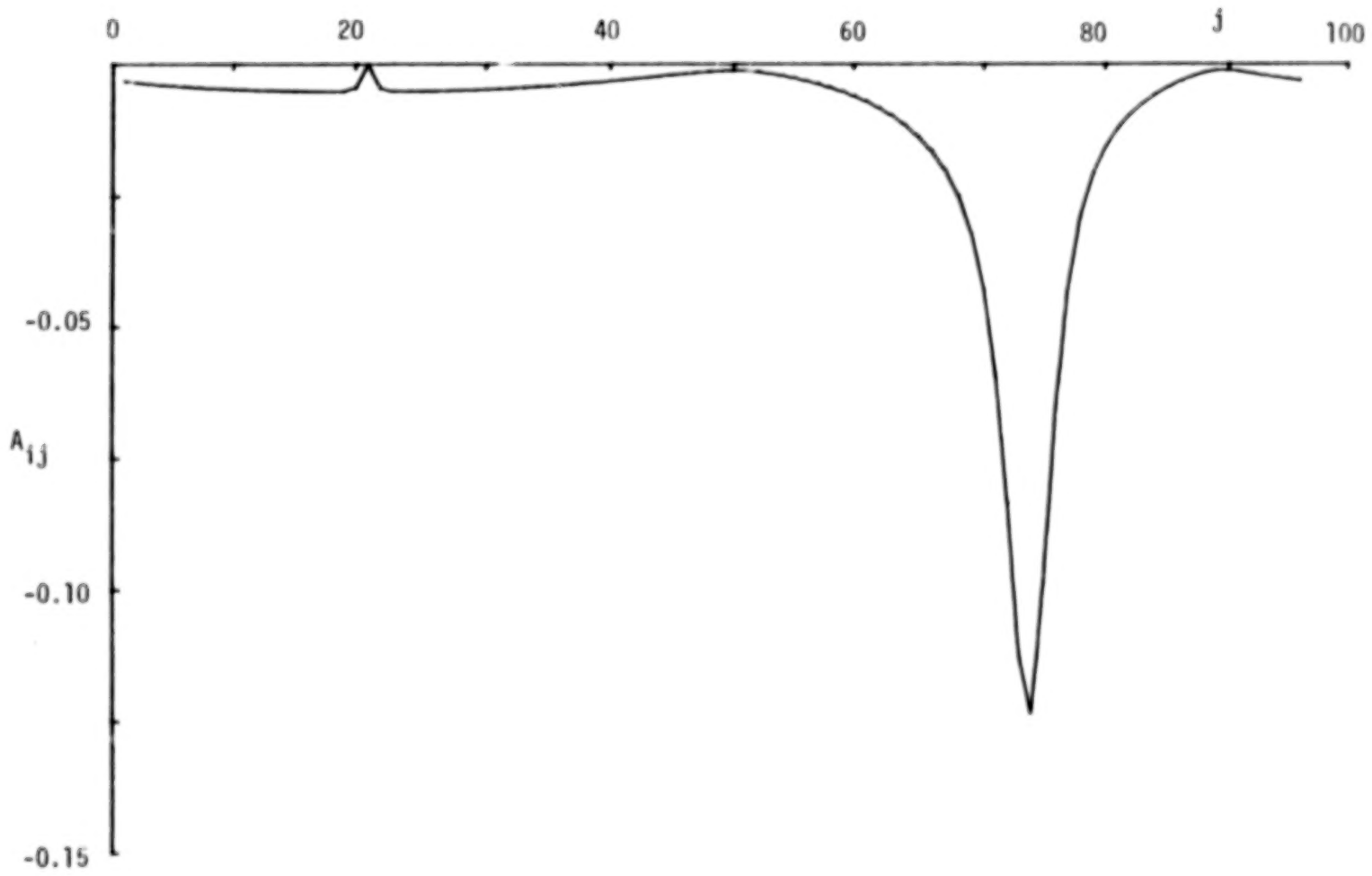

Figure 6. The behavior of A_{ij} matrix for $i = 21$ on the 96-point E33 airfoil.

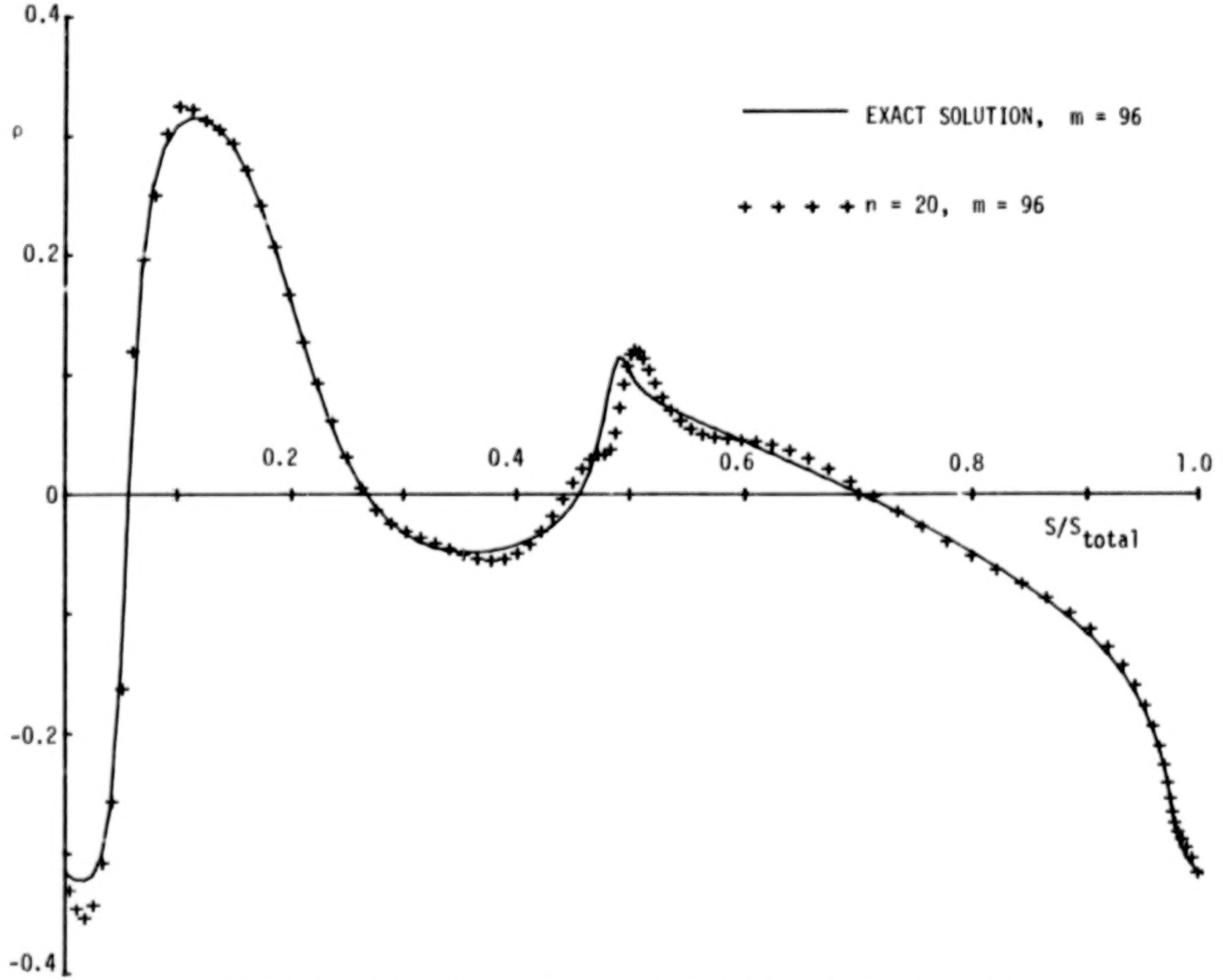

Figure 7. Source distribution for E33 airfoil; eigenvector method.

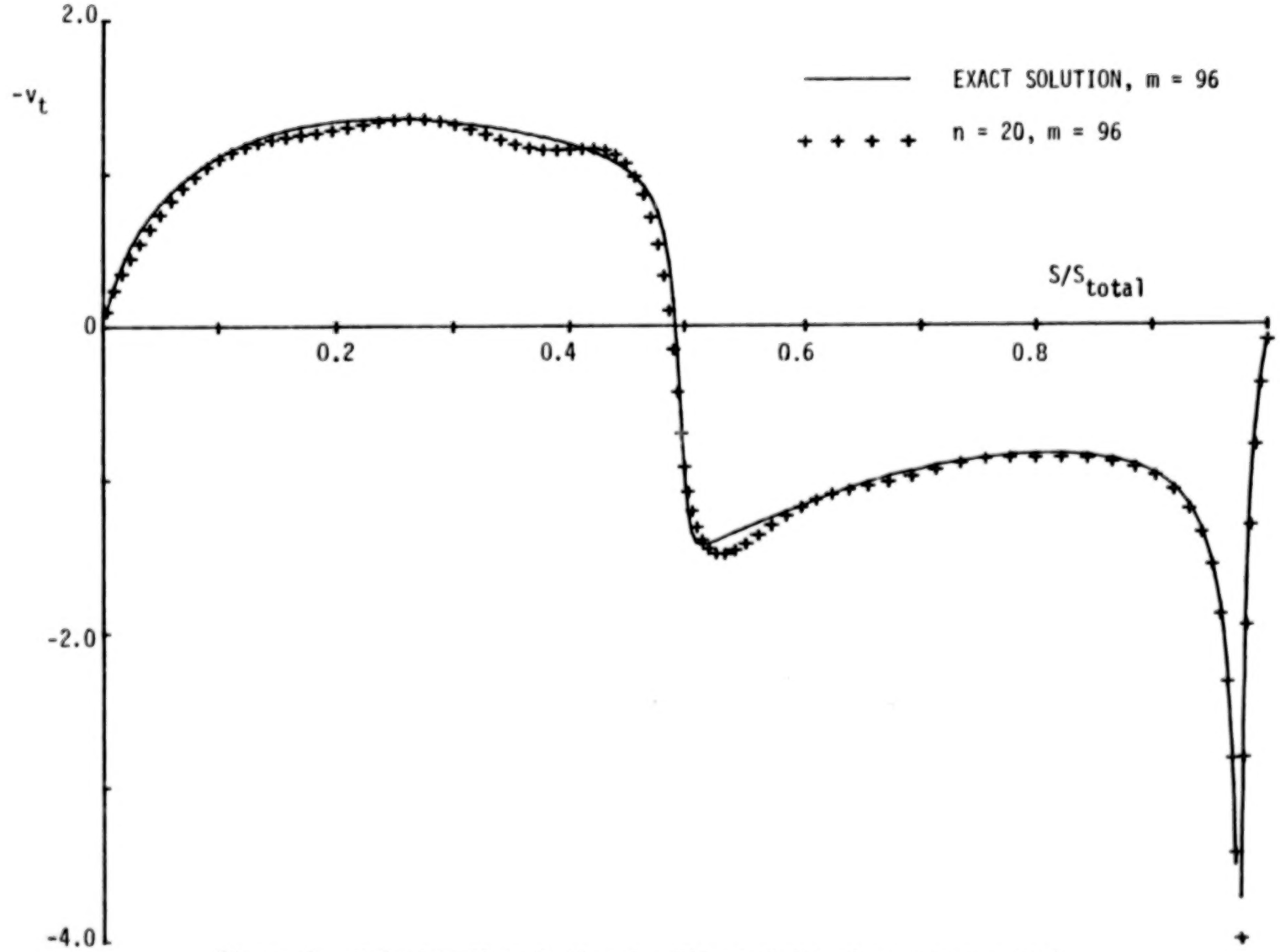

Figure 8. Velocity distribution for E33 airfoil; eigenvector method.

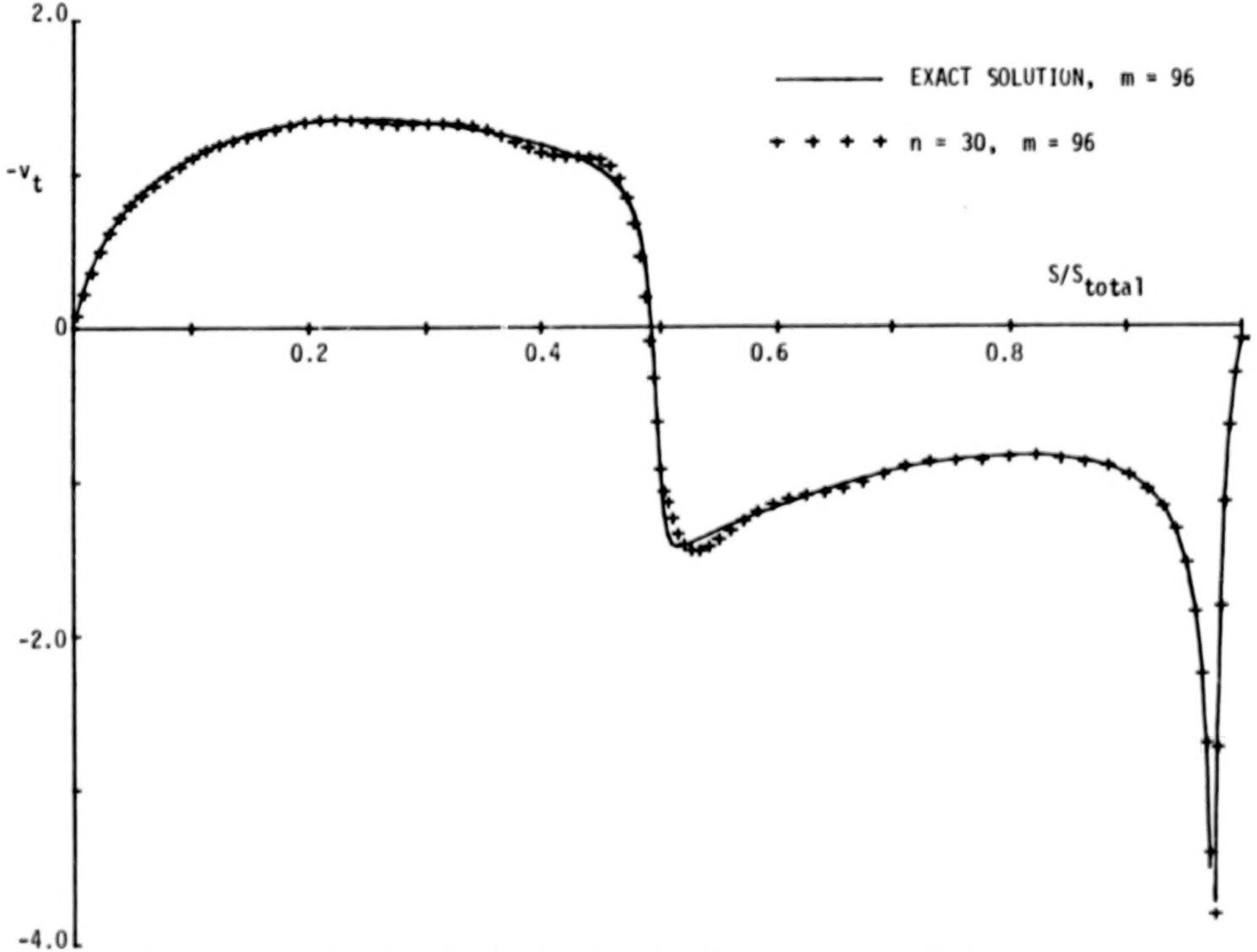

Figure 9. Velocity distribution for E33 airfoil; eigenvector method.

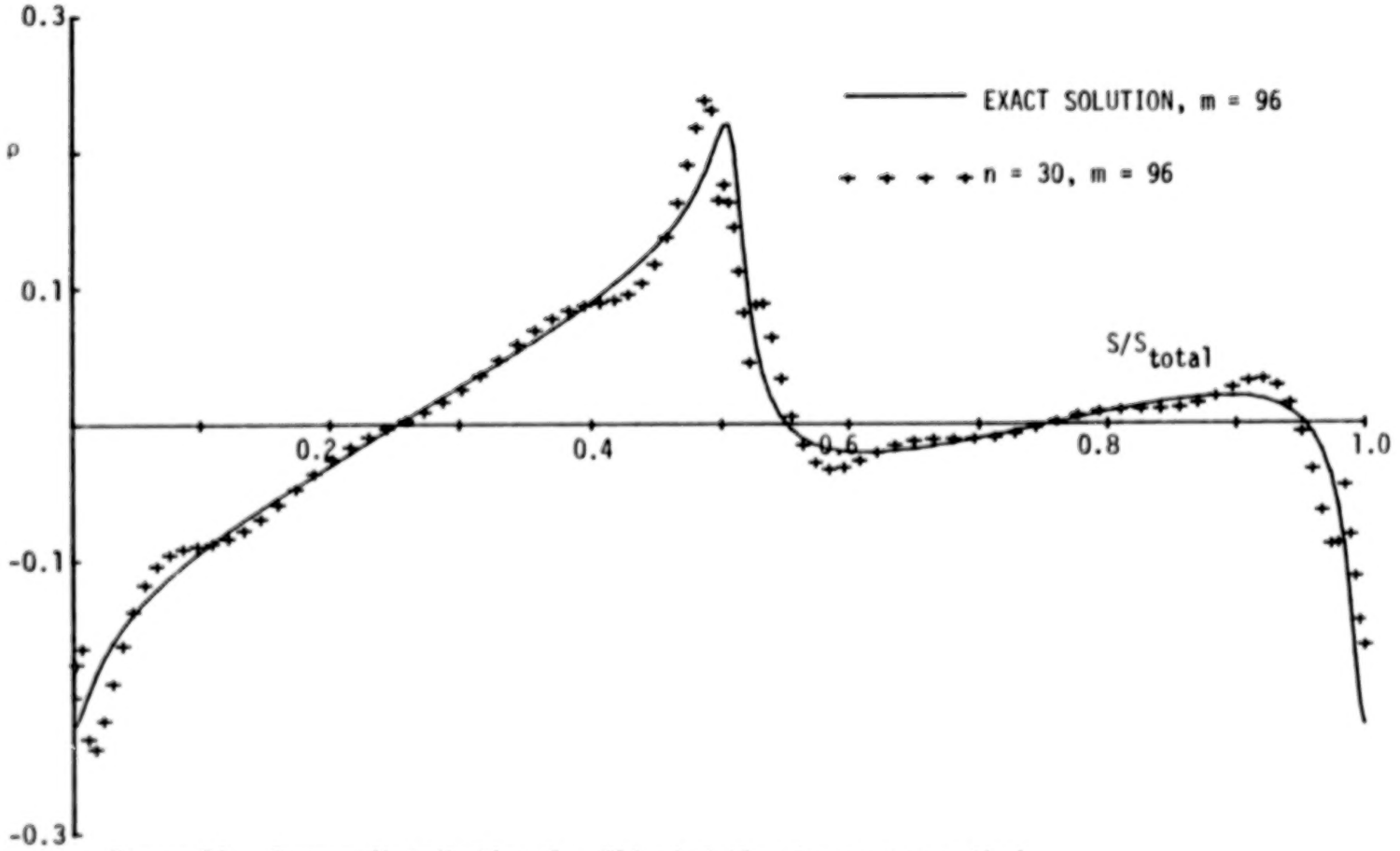

Figure 10. Source distribution for E13 airfoil; eigenvector method.

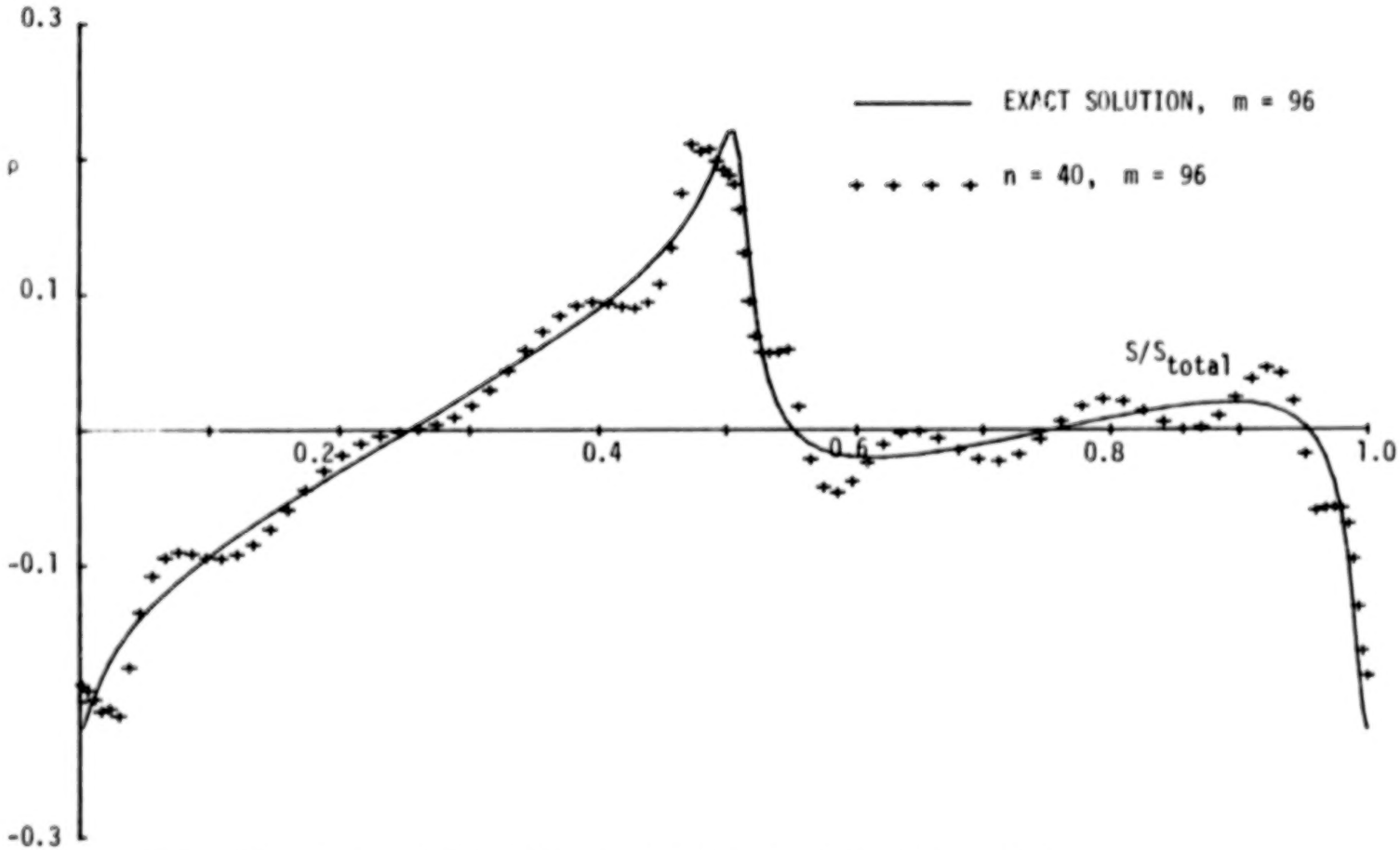

Figure 11. Source distribution for E13 airfoil; eigenvector method.

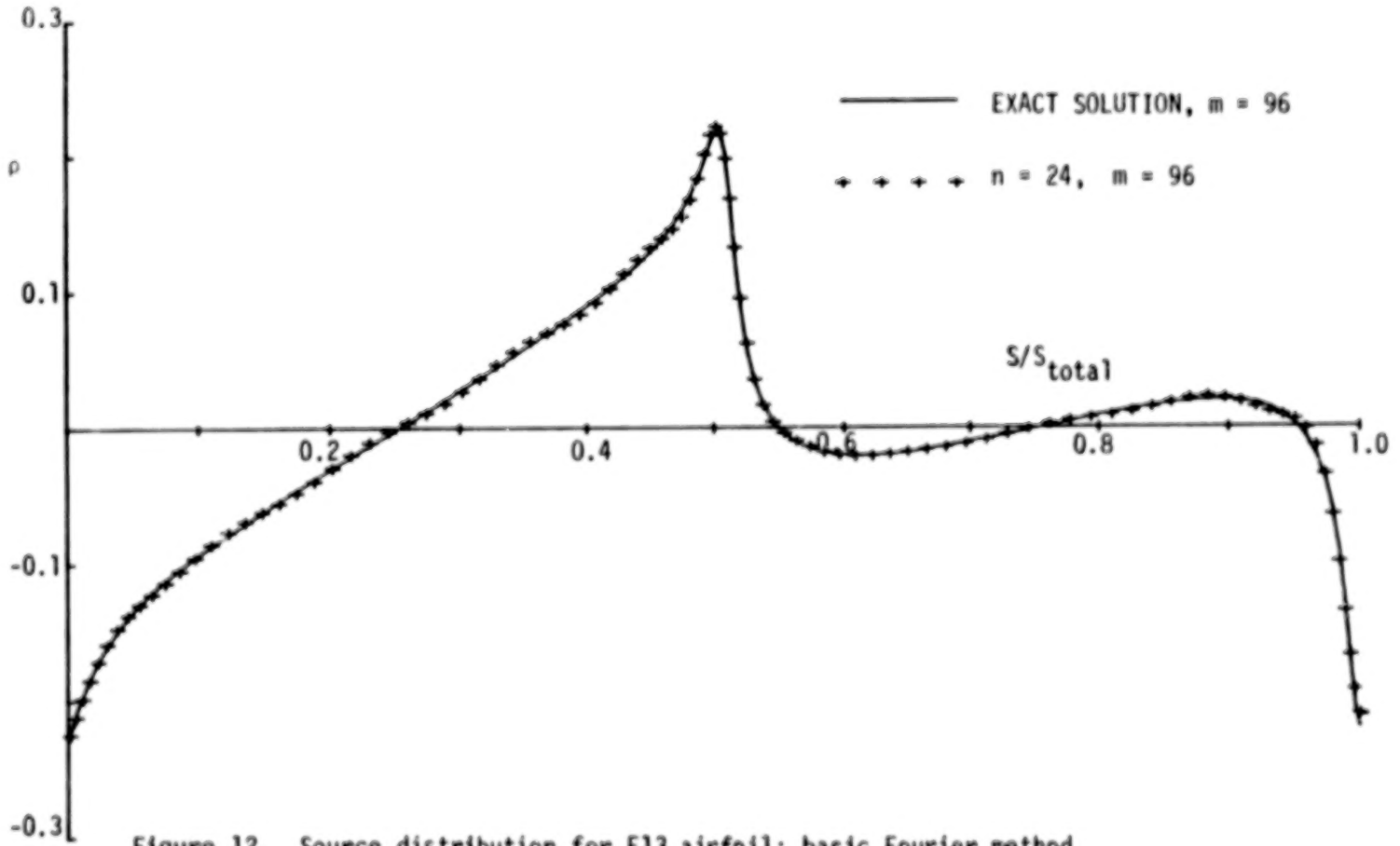

Figure 12. Source distribution for E13 airfoil; basic Fourier method.

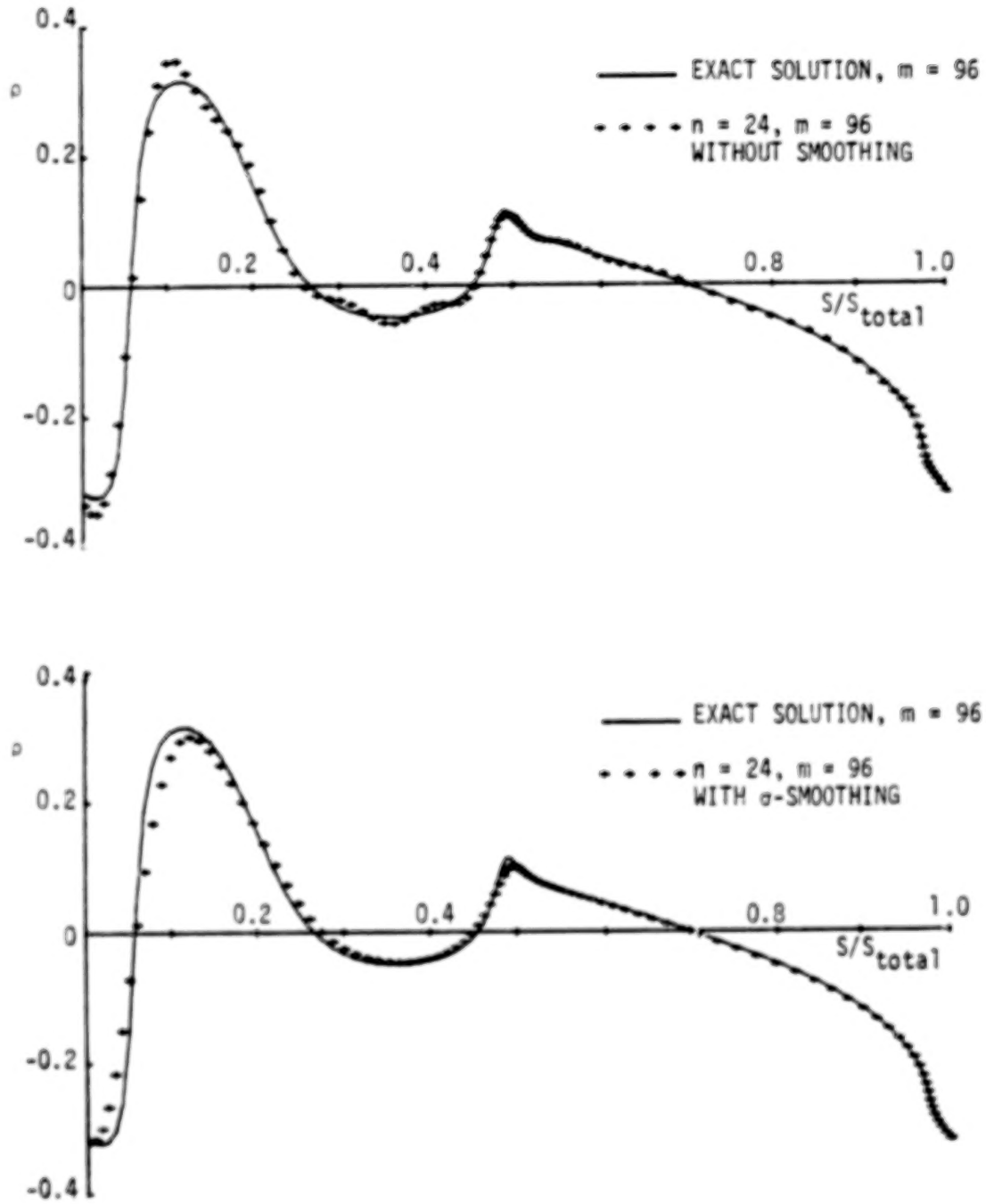

Figure 13. Source distribution for E33 airfoil; basic Fourier method with and without σ-smoothing.

BLANK

PAGE

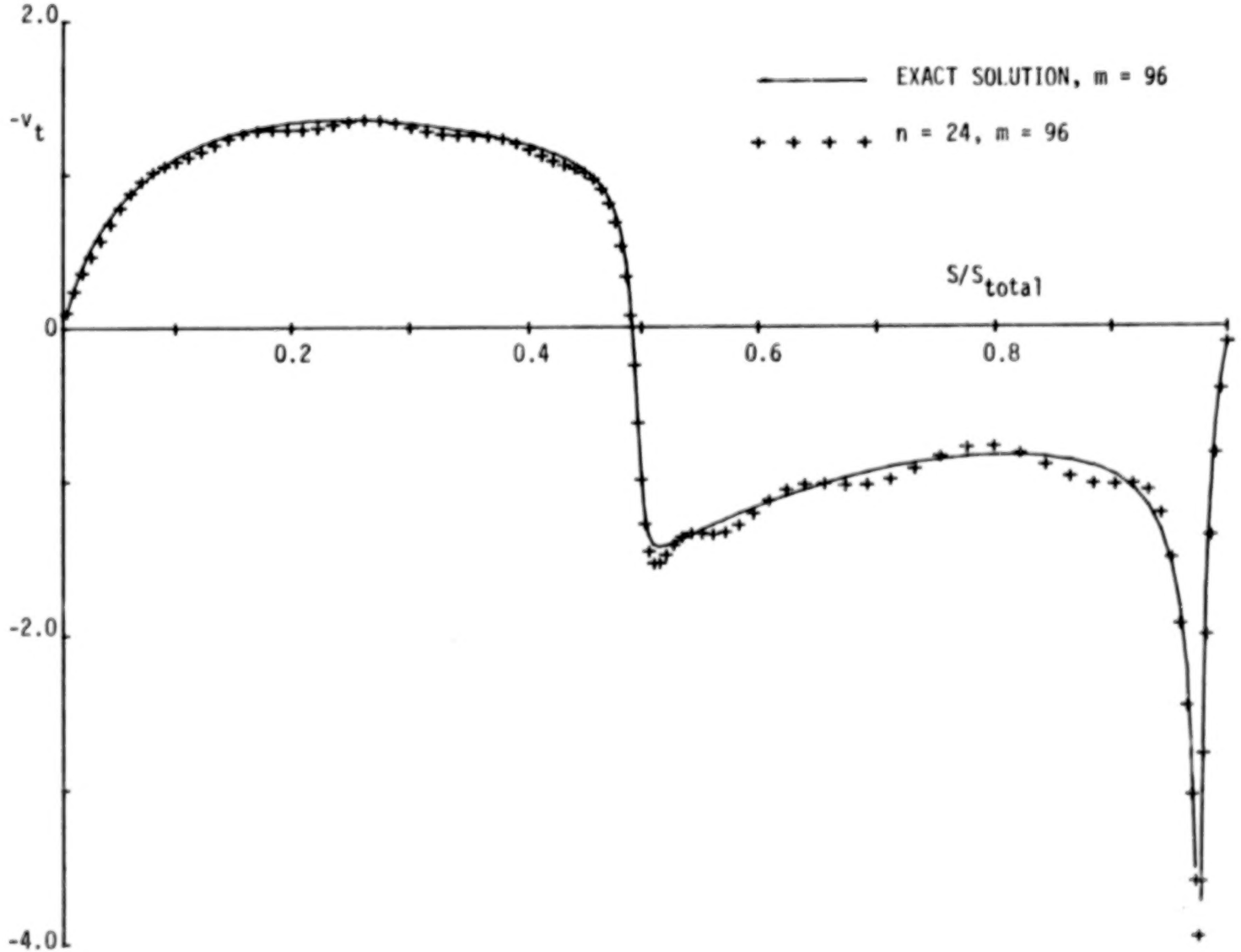

Figure 14. Velocity distribution for E33 airfoil; basic Fourier method.

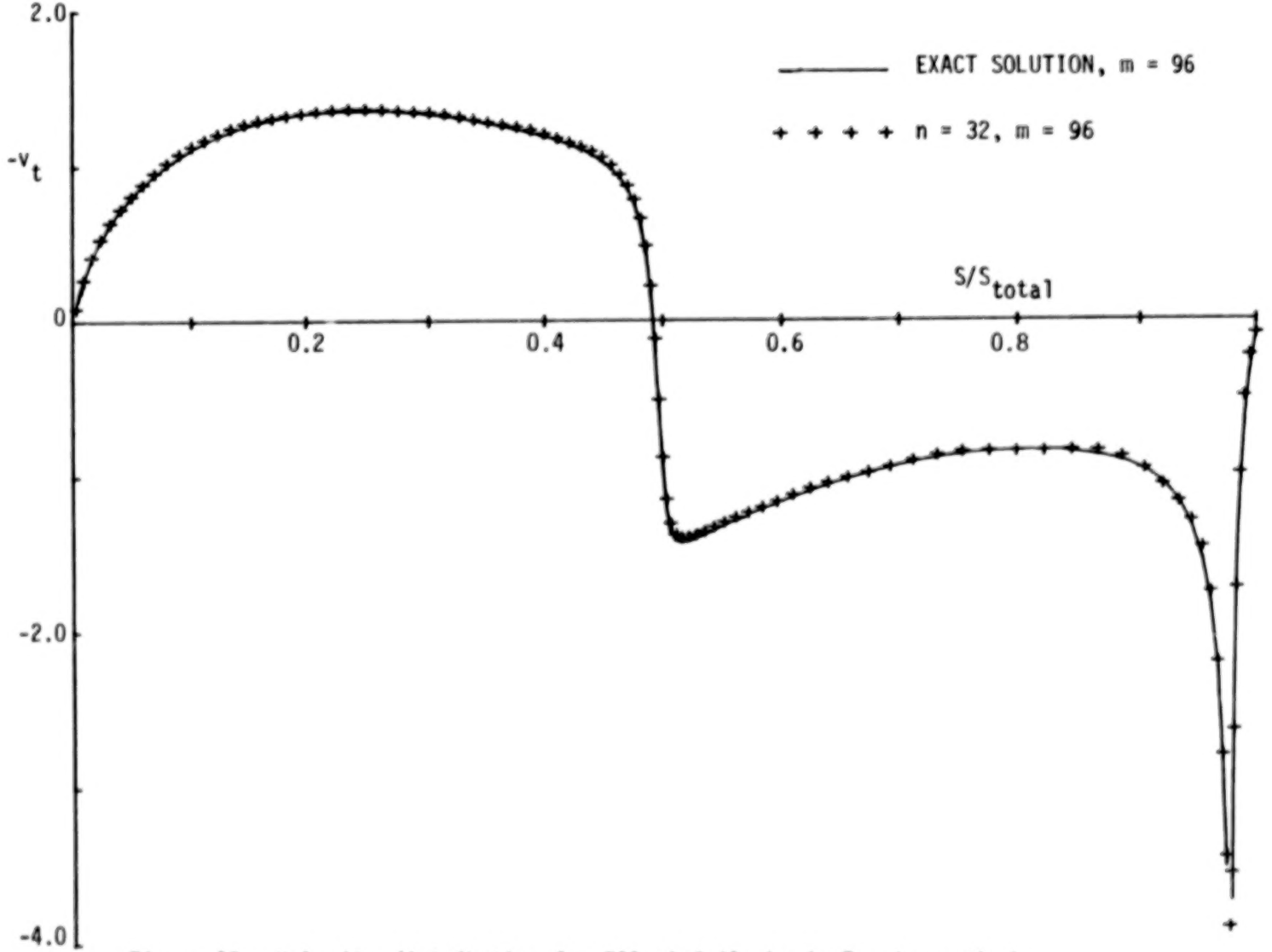

Figure 15. Velocity distribution for E33 airfoil; basic Fourier method.

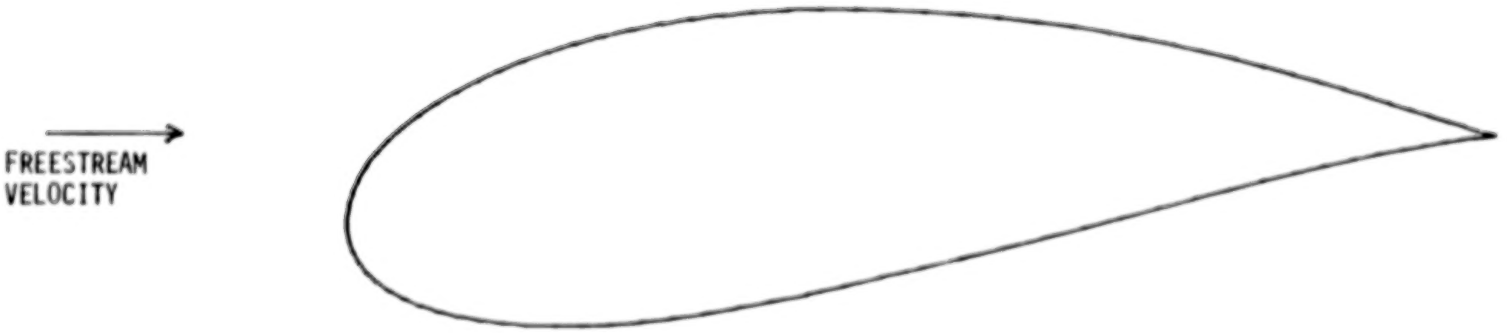

Figure 16. The BCC#2 airfoil.

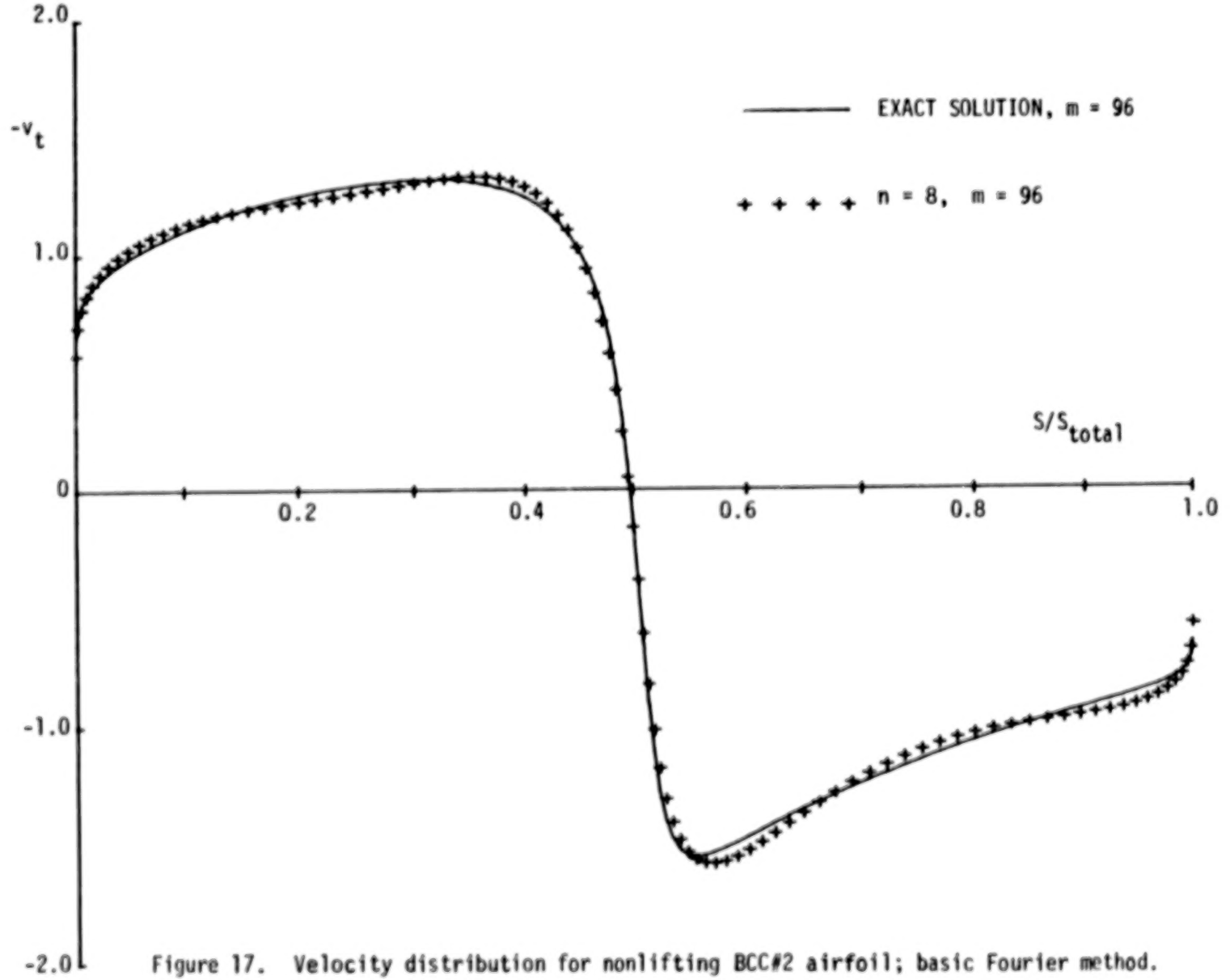

Figure 17. Velocity distribution for nonlifting BCC#2 airfoil; basic Fourier method.

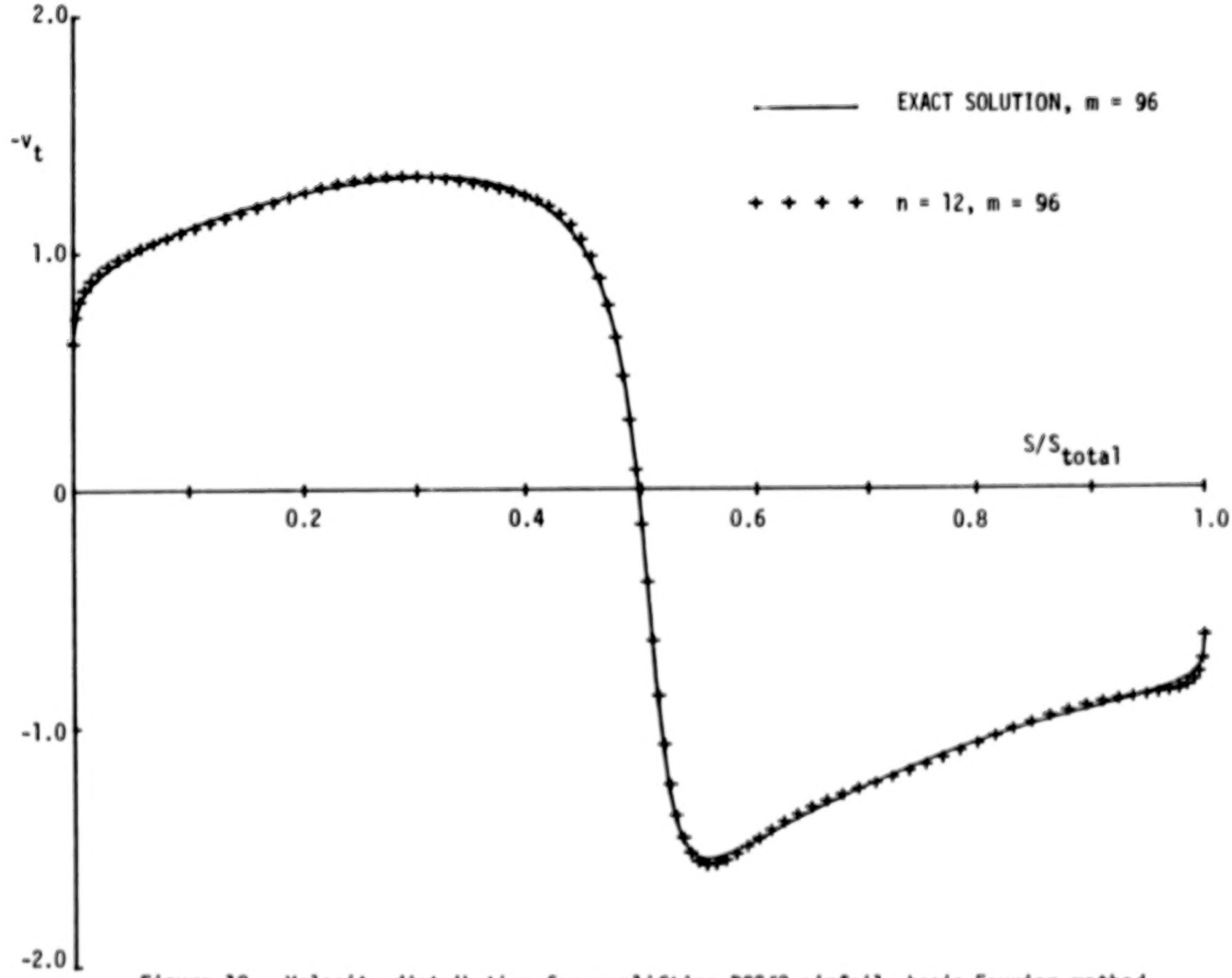

Figure 18. Velocity distribution for nonlifting BCC#2 airfoil; basic Fourier method.

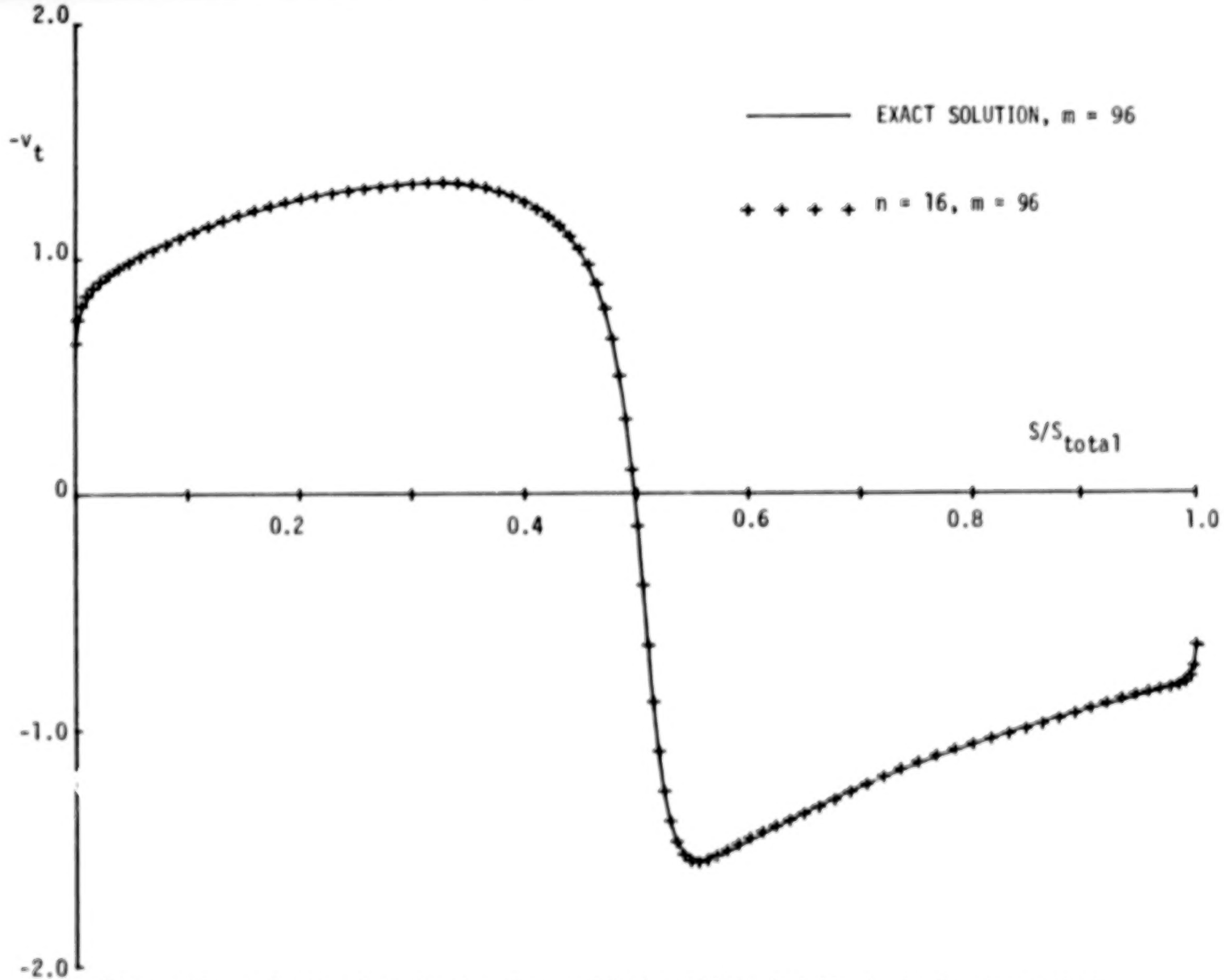

Figure 19. Velocity distribution for nonlifting BCC#2 airfoil; basic Fourier method.

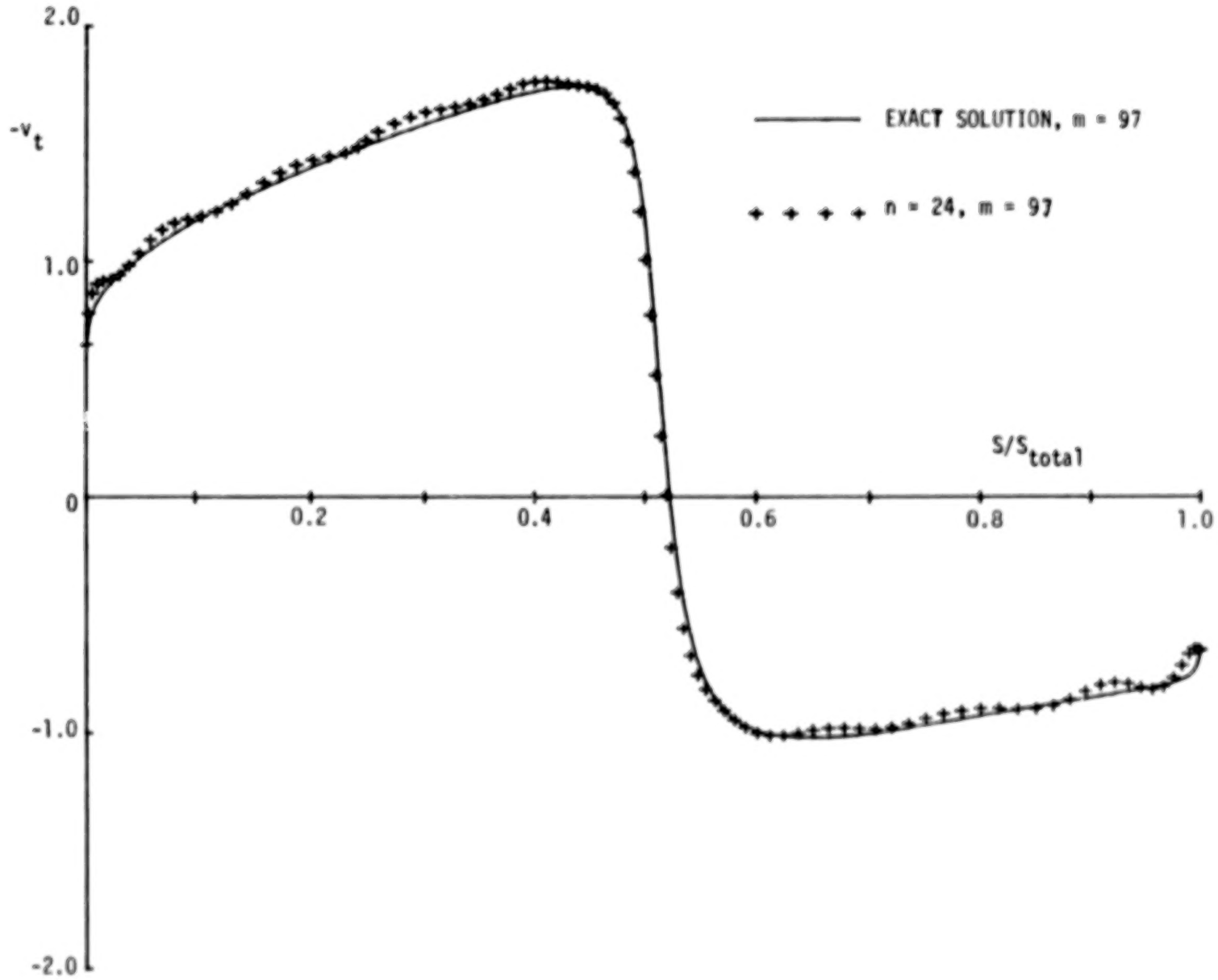

Figure 20. Velocity distribution for lifting BCC#2 airfoil (α = 10°); Fourier method with linear fit.

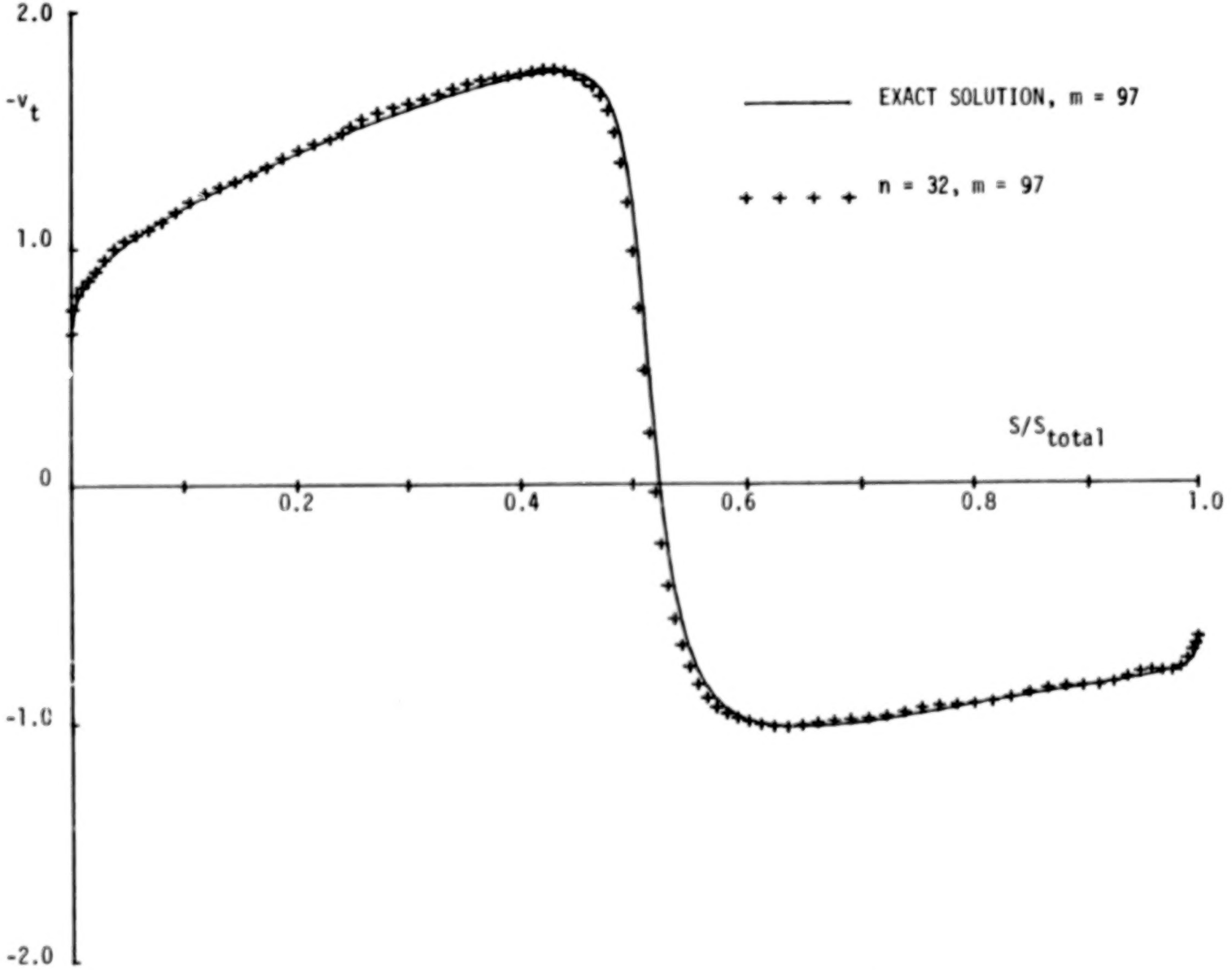

Figure 21. Velocity distribution for lifting BCC#2 airfoil (α = 10°); Fourier method with linear fit.

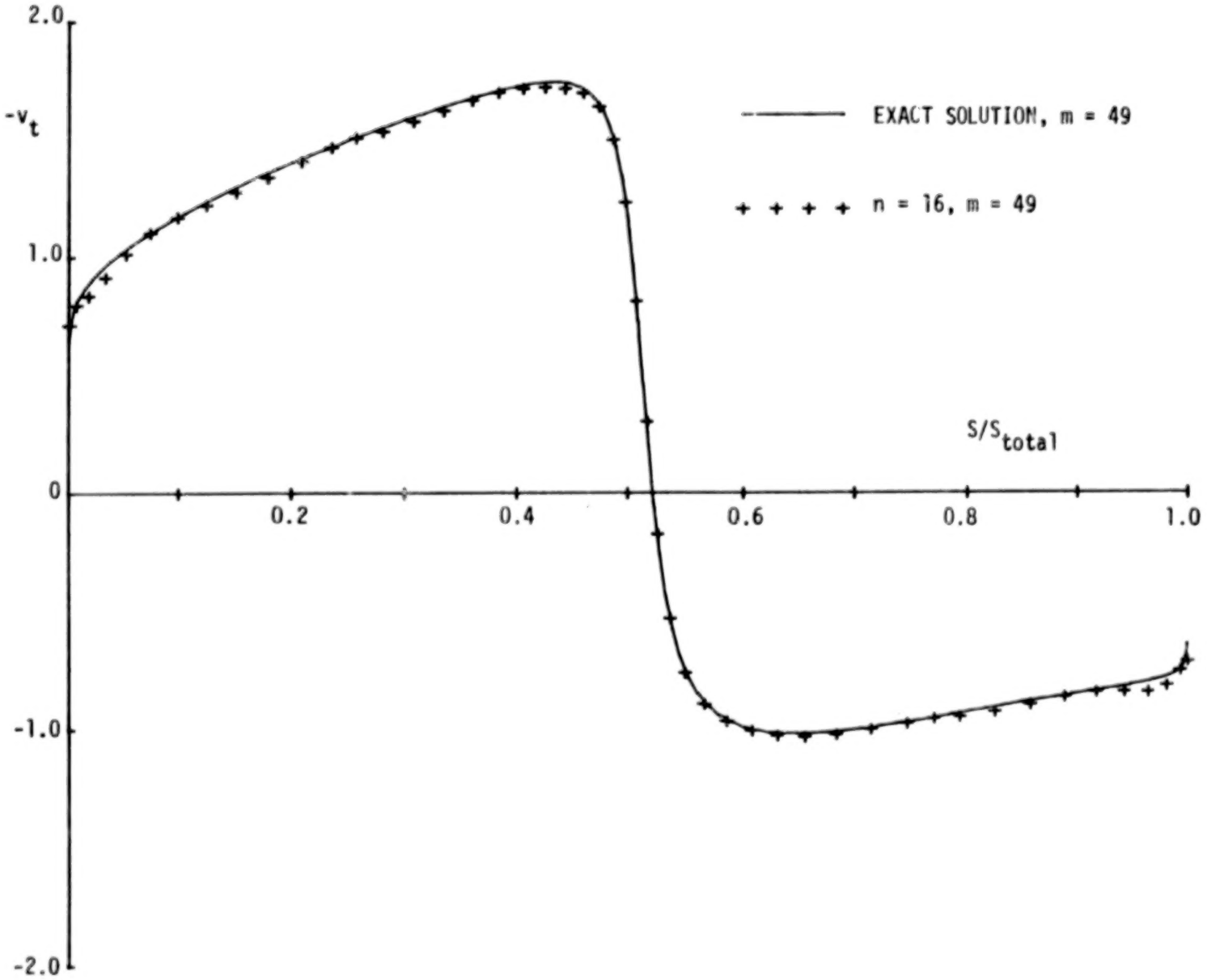

Figure 22. Velocity distribution for lifting BCC#2 airfoil (α = 10°); Fourier method with singular fit.

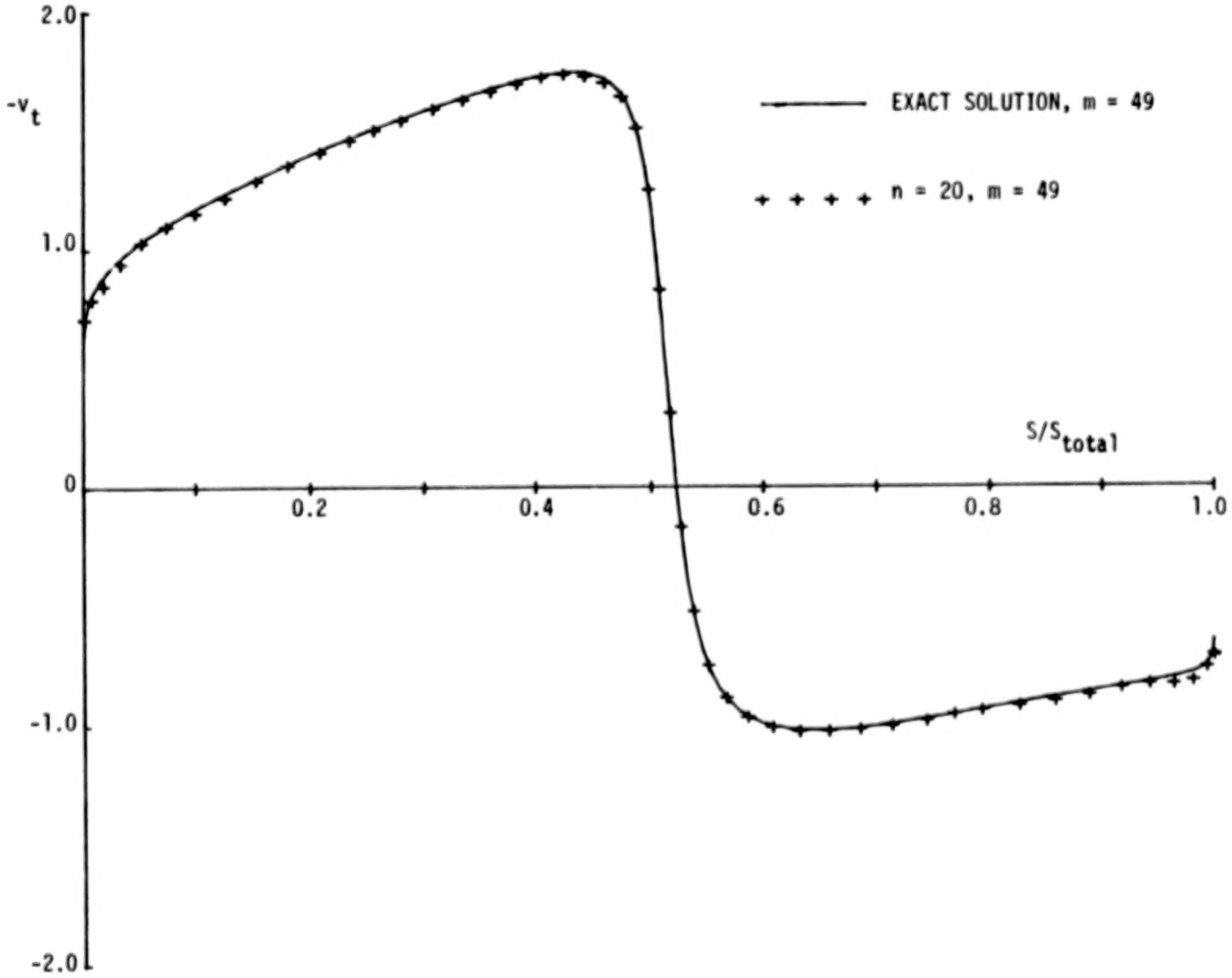

Figure 23. Velocity distribution for lifting BCC#2 airfoil (α = 10°); Fourier method with singular fit.

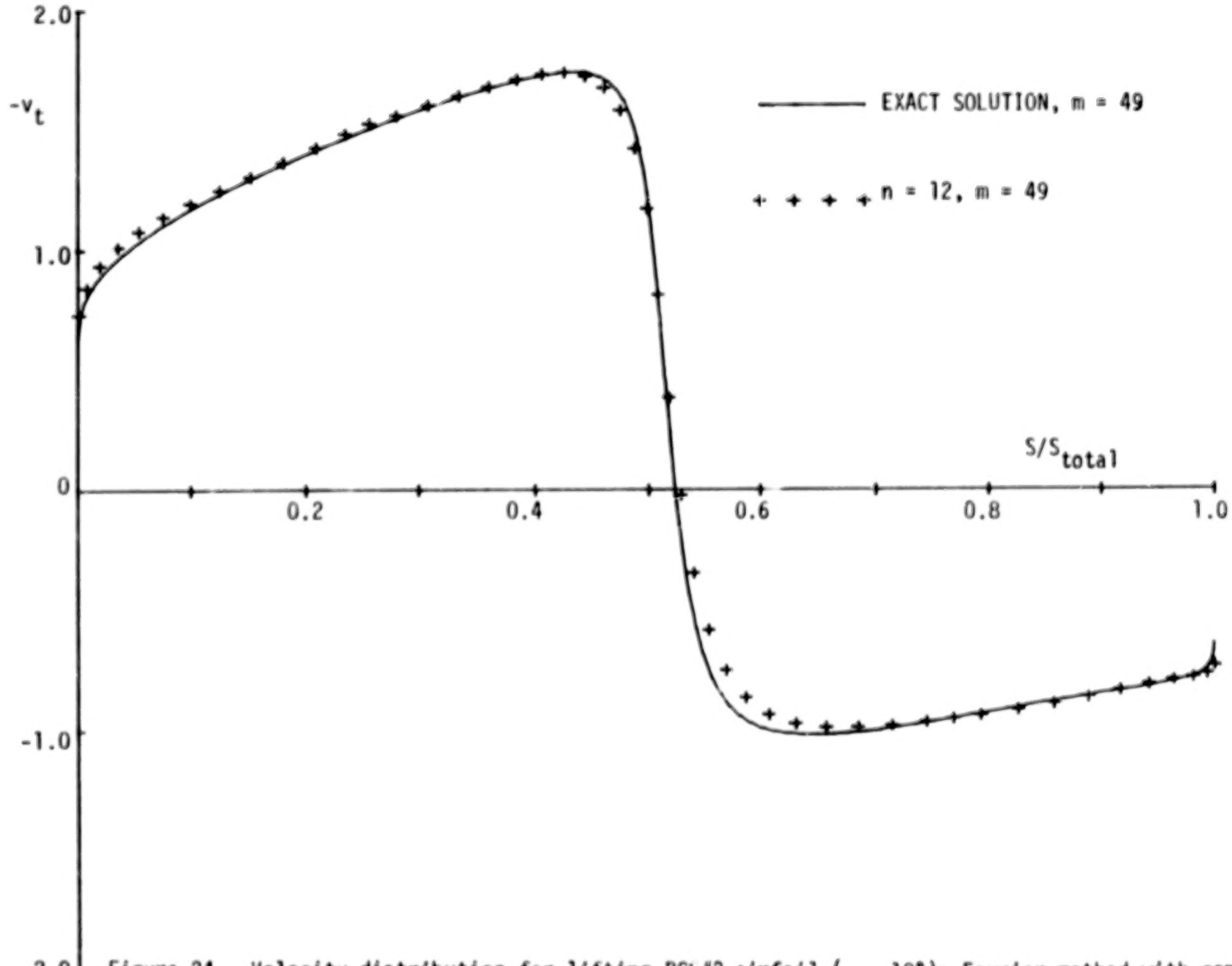

Figure 24. Velocity distribution for lifting BCAR2 airfoil (α = 10°); Fourier method with combined Kutta condition, linear fit and σ-smoothing.

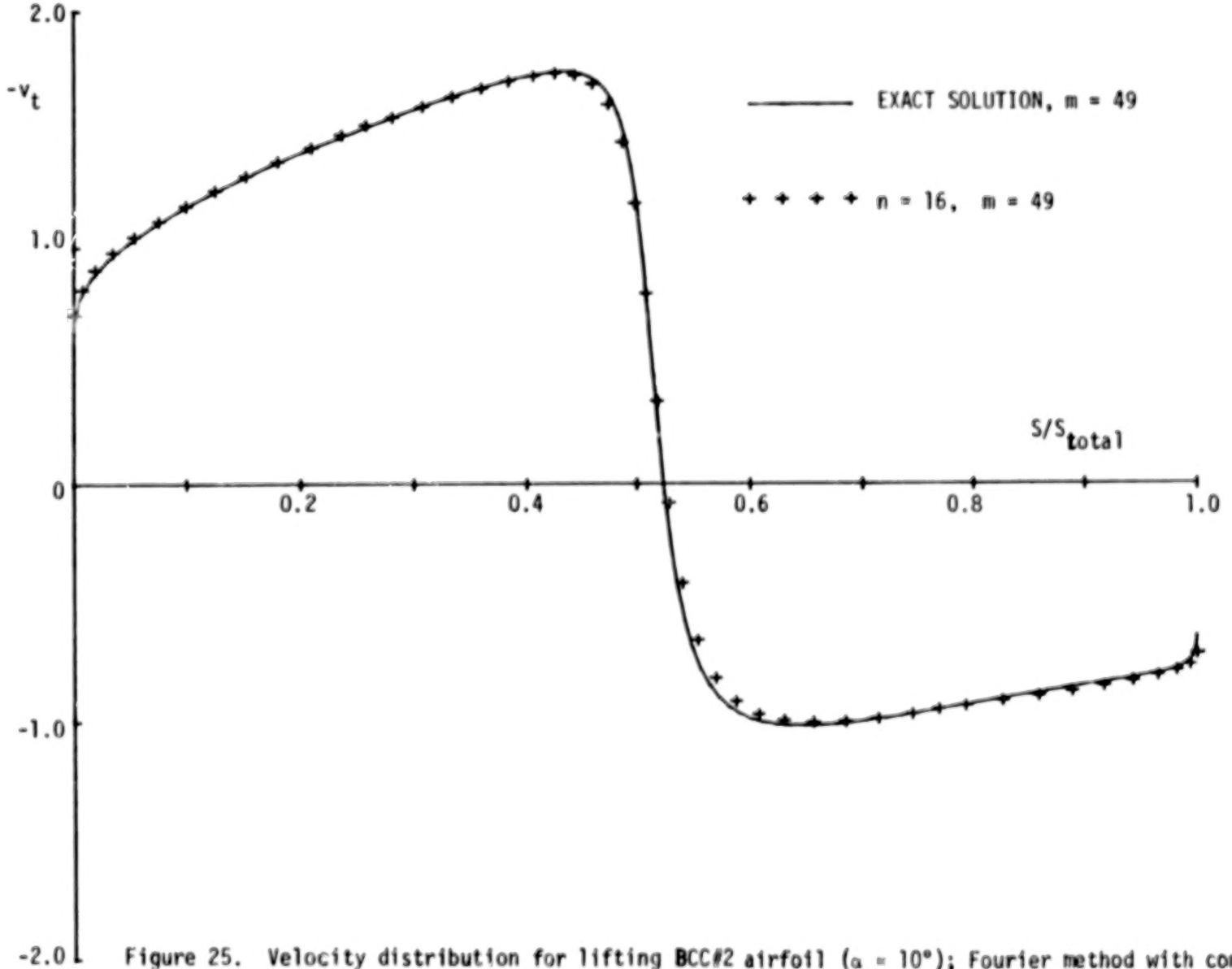

Figure 25. Velocity distribution for lifting BCC#2 airfoil (α = 10°); Fourier method with combined Kutta condition, linear fit and σ-smoothing.

FREESTREAM
VELOCITY

Figure 26. Thin lifting airfoil ($\alpha = 5°$).

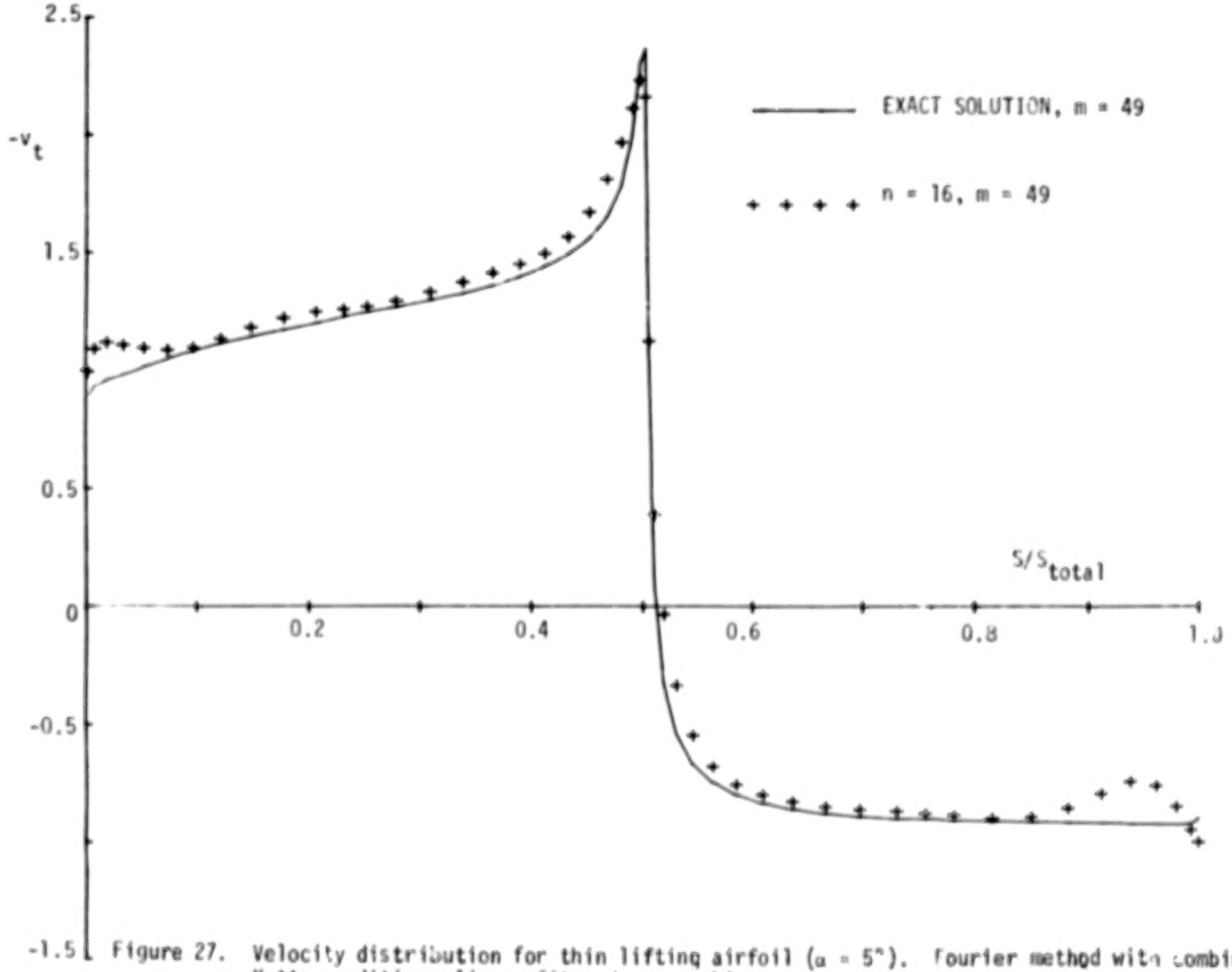

Figure 27. Velocity distribution for thin lifting airfoil ($\alpha = 5°$). Fourier method with combined Kutta condition, linear fit and σ-smoothing.

TABLE OF CONTENTS

BLANK

PAGE

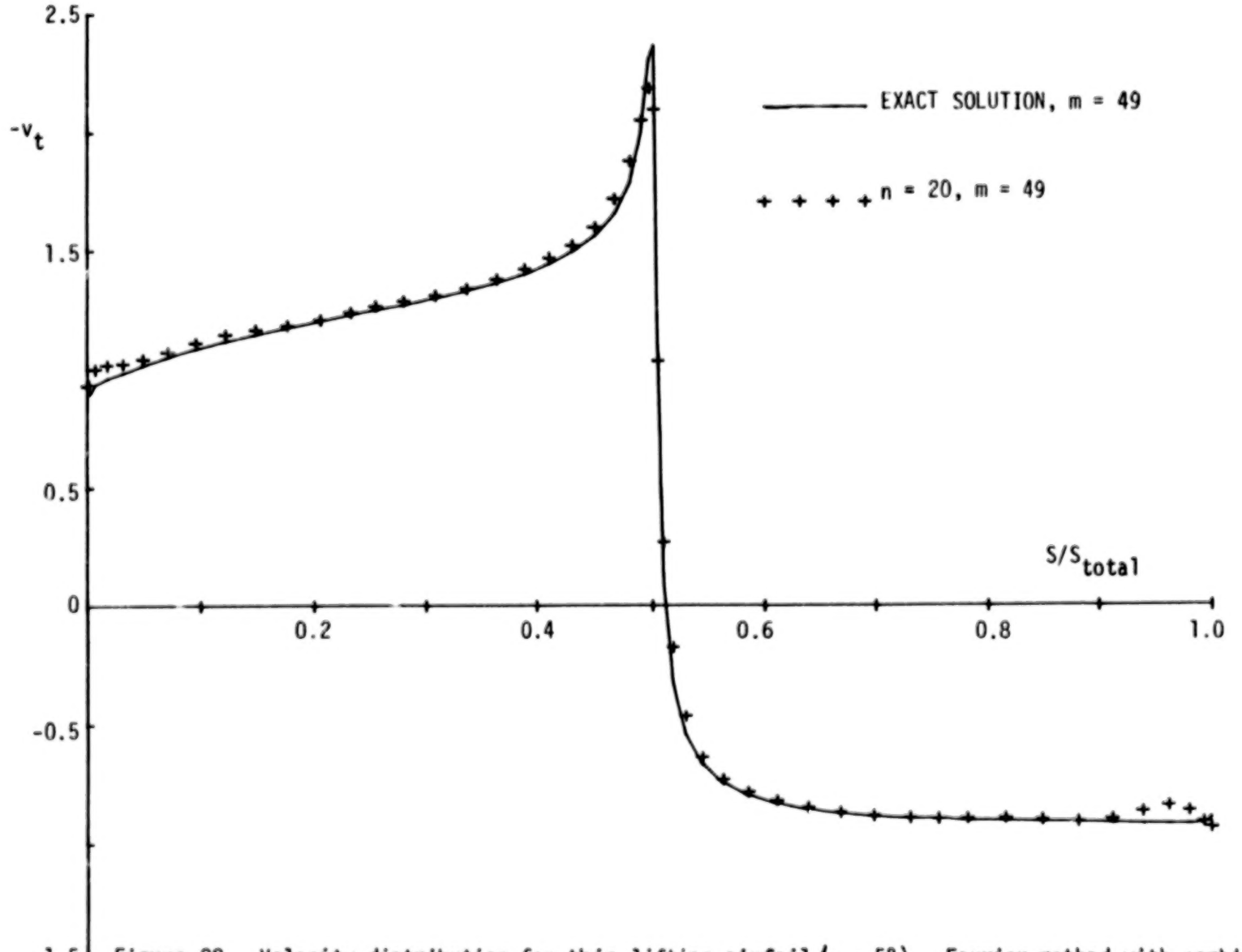

Figure 28. Velocity distribution for thin lifting airfoil ($\alpha = 5°$). Fourier method with combined Kutta conditions, linear fit and σ-smoothing.

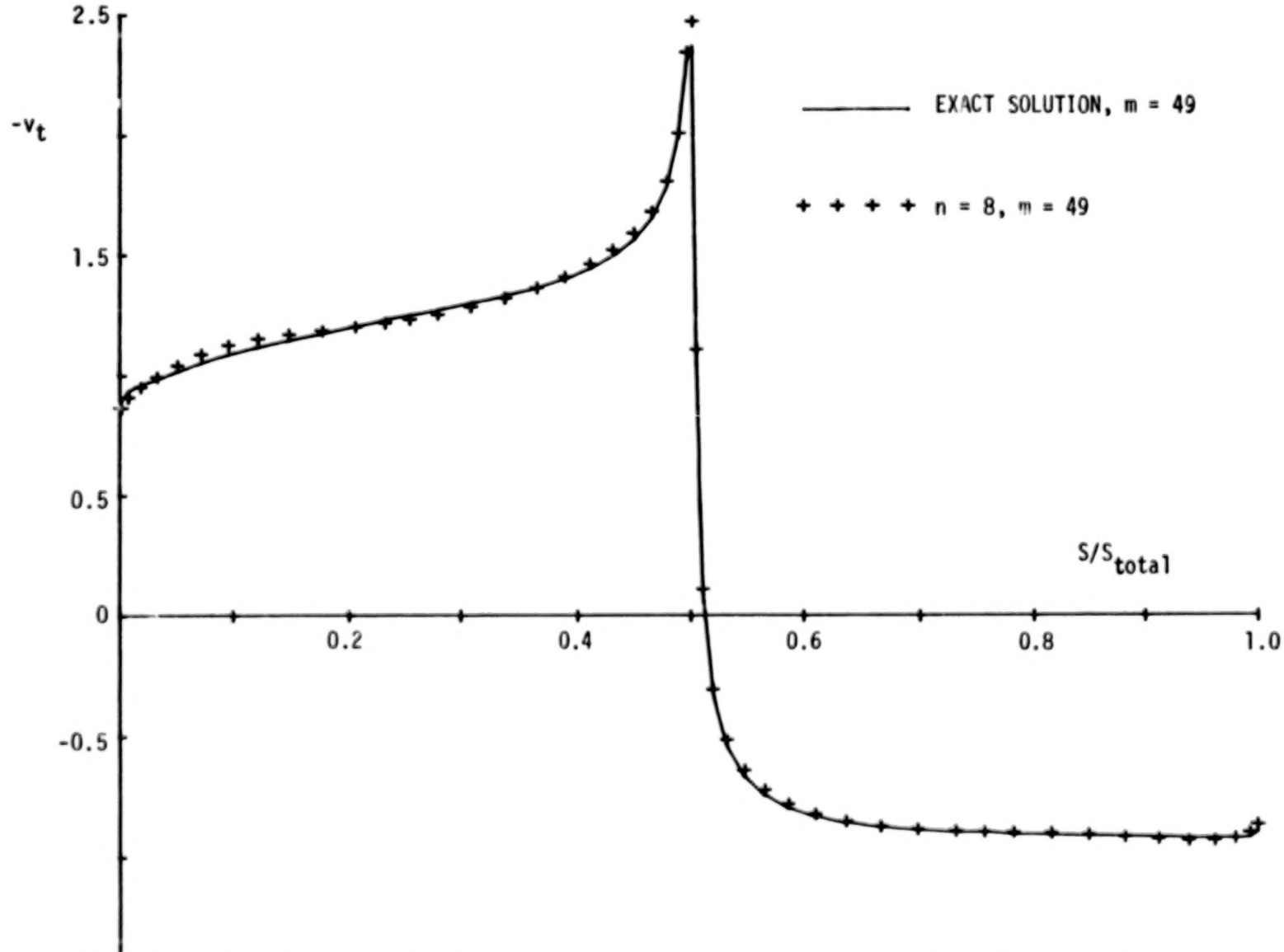

Figure 29. Velocity distribution for thin lifting airfoil ($\alpha = 5°$). Fourier method with improved matrix truncation scheme and linear fit.

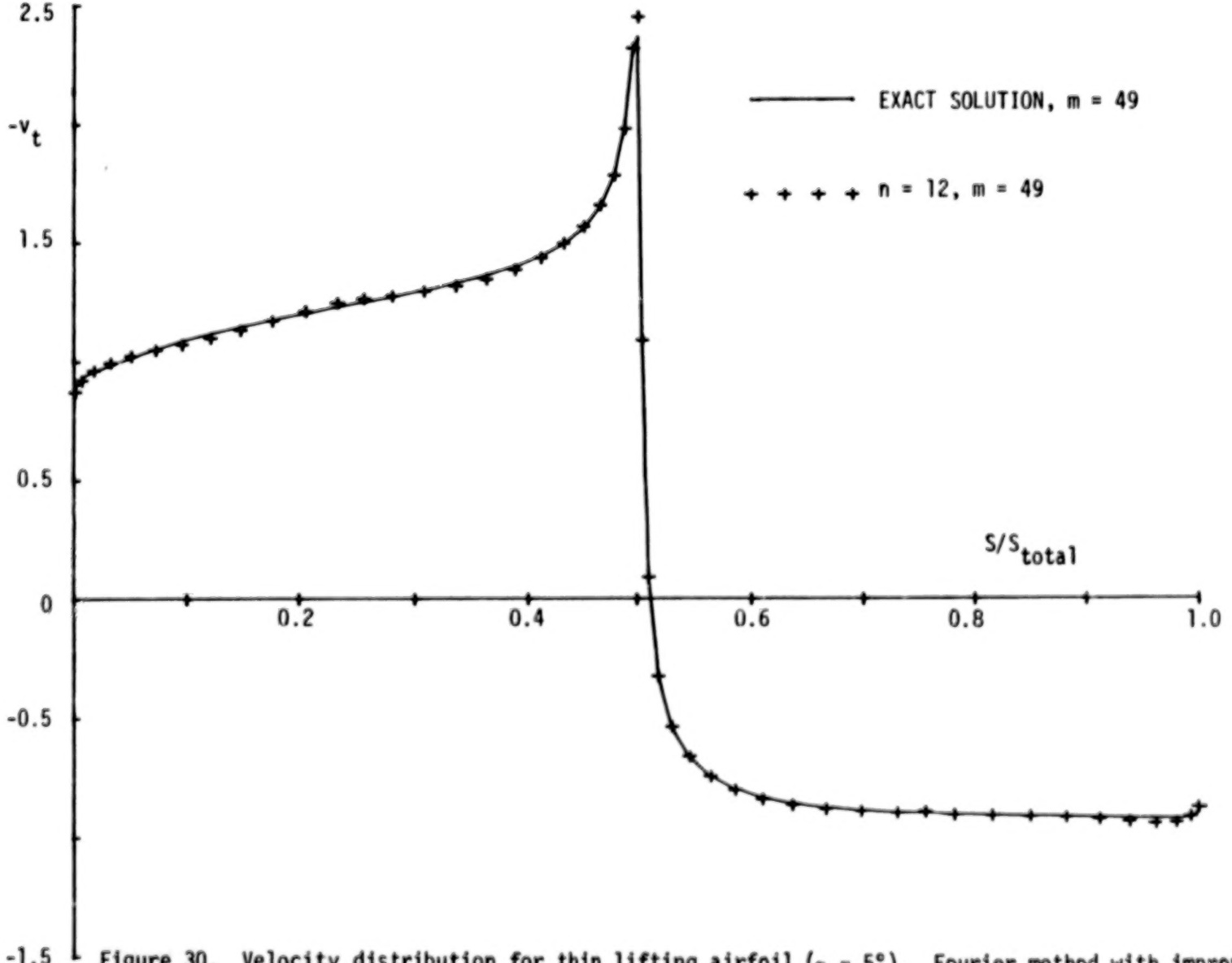

Figure 30. Velocity distribution for thin lifting airfoil ($\alpha = 5°$). Fourier method with improved matrix truncation scheme and linear fit.

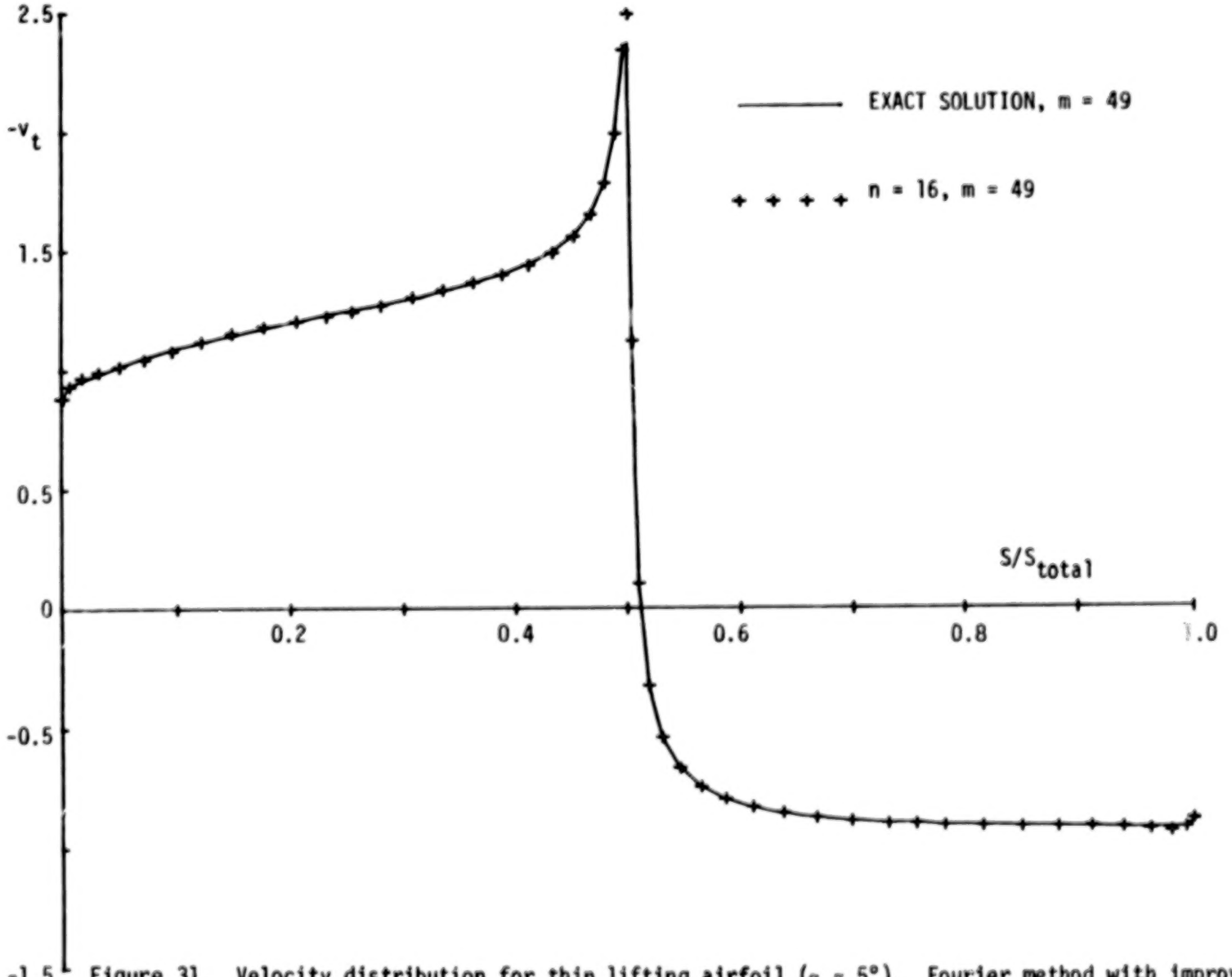

Figure 31. Velocity distribution for thin lifting airfoil ($\alpha = 5°$). Fourier method with improved matrix truncation scheme and linear fit.

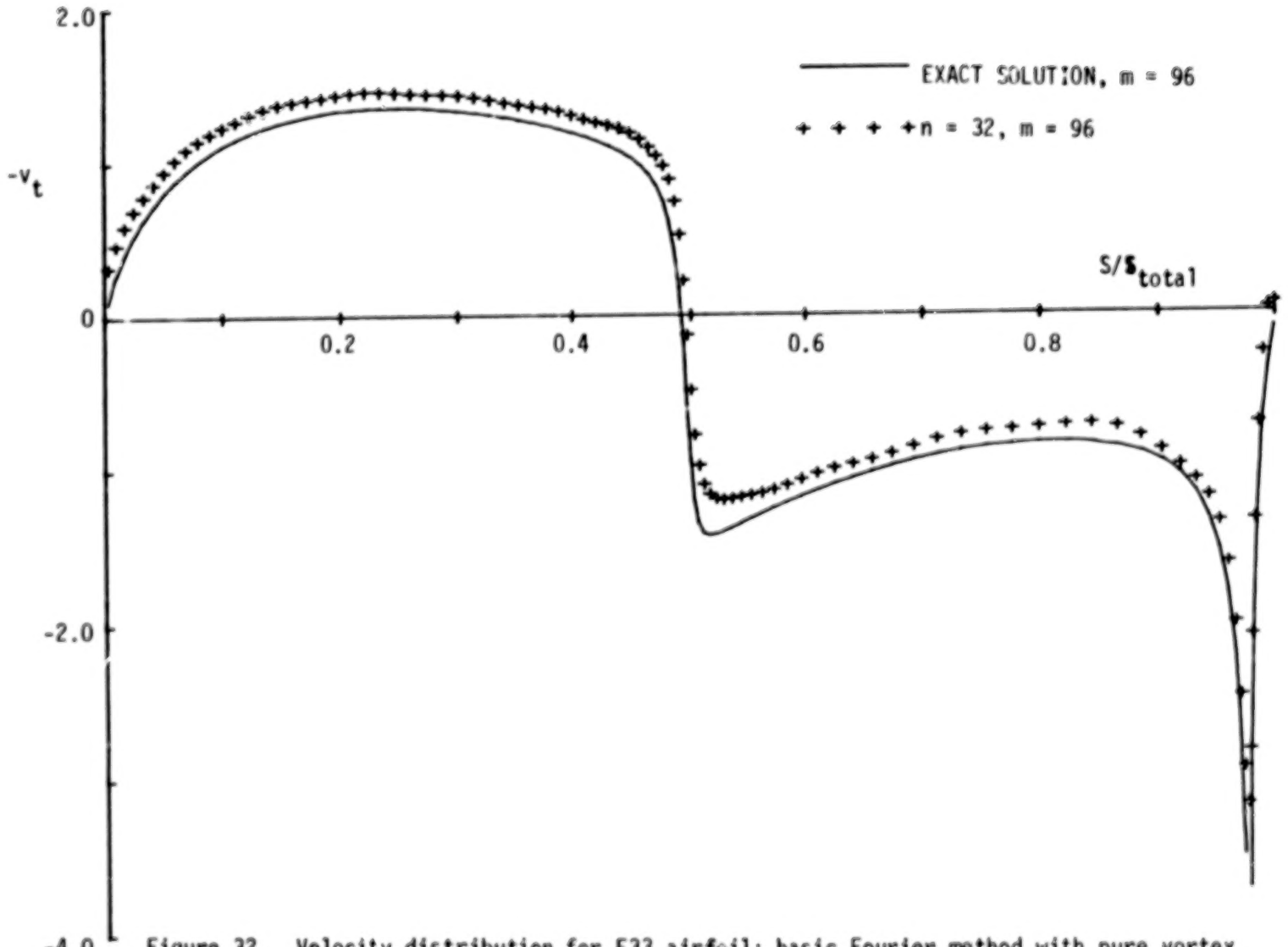

Figure 32. Velocity distribution for E33 airfoil; basic Fourier method with pure vortex distribution and external normal-velocity condition.

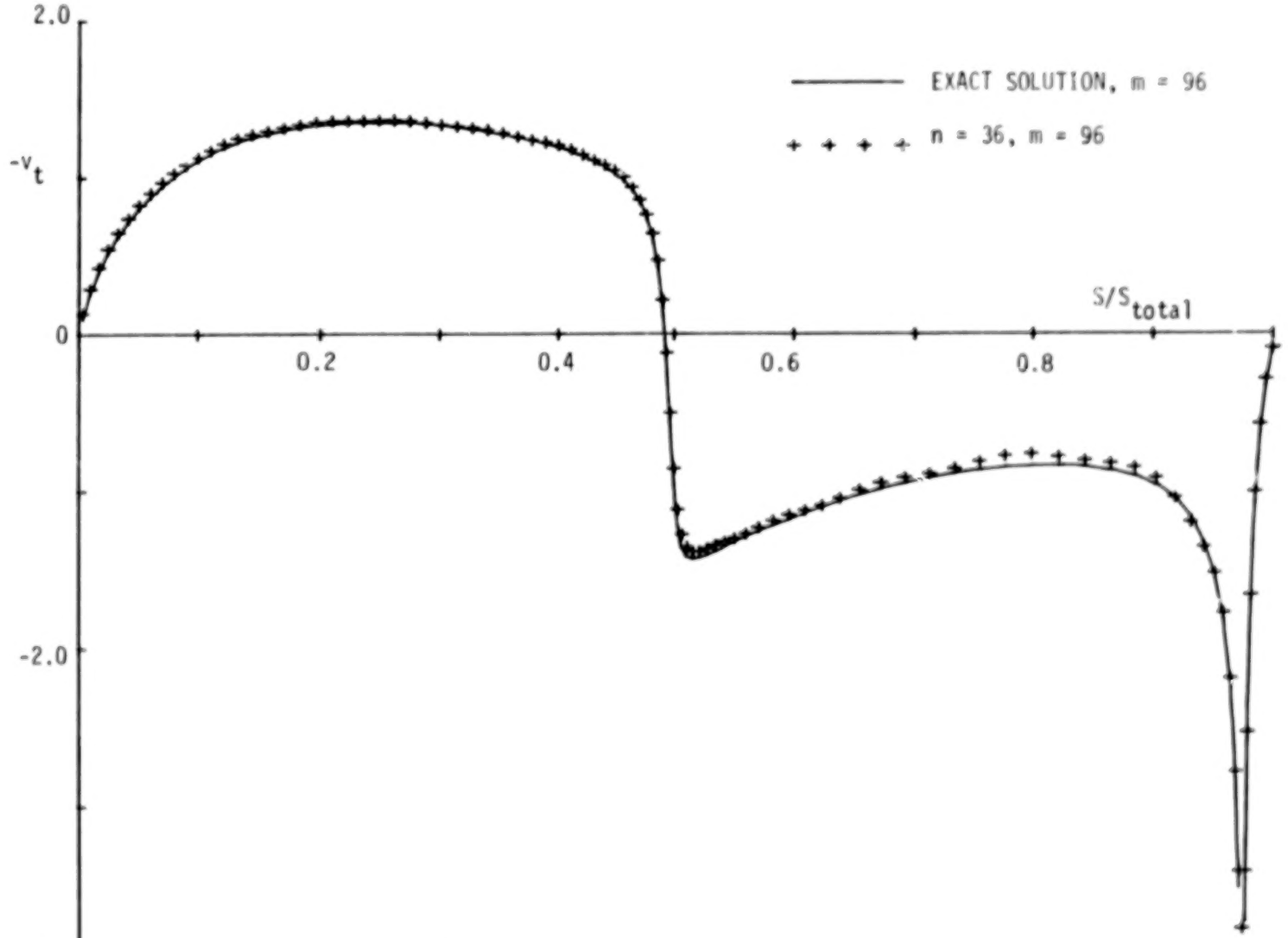

Figure 33. Velocity distribution for E33 airfoil; basic Fourier method with pure vortex distribution and external normal-velocity condition.

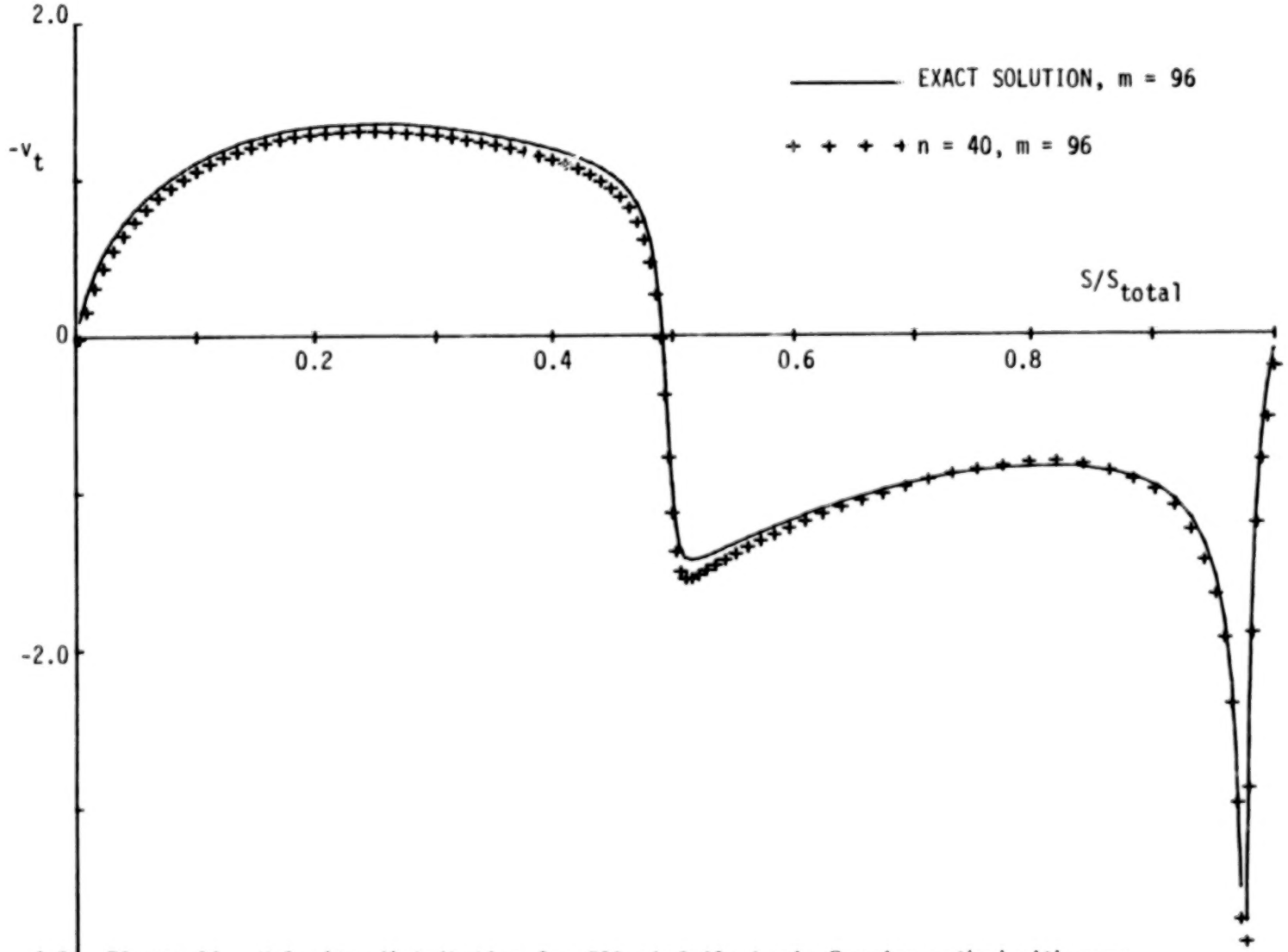

Figure 34. Velocity distribution for E33 airfoil; basic Fourier method with pure vortex distribution and external normal-velocity condition.

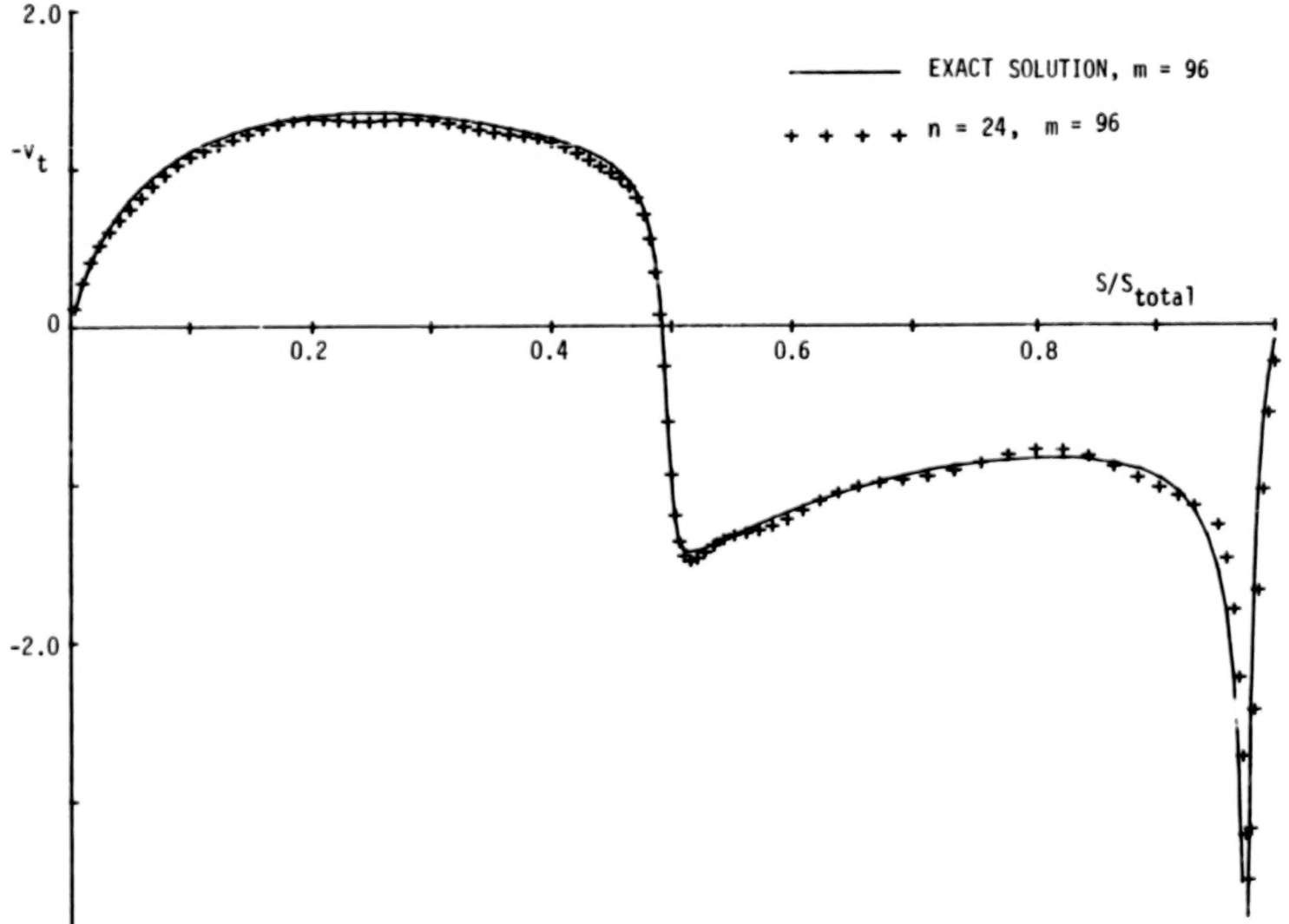

Figure 35. Velocity distribution for E33 airfoil; basic Fourier method with pure vortex distribution and internal tangential-velocity condition.

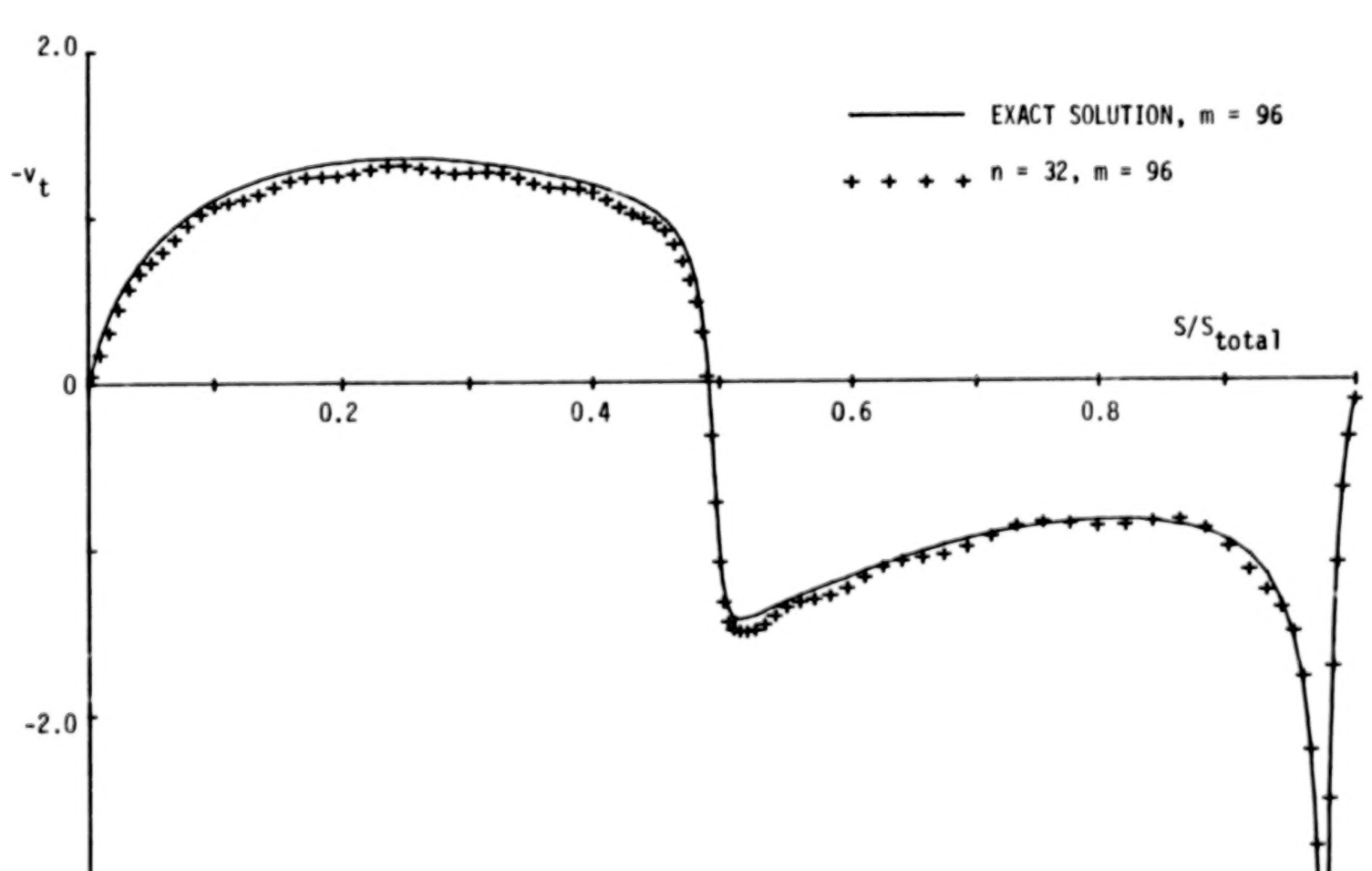

Figure 36. Velocity distribution for E33 airfoil; basic Fourier method with pure vortex distribution and internal tangential-velocity condition.

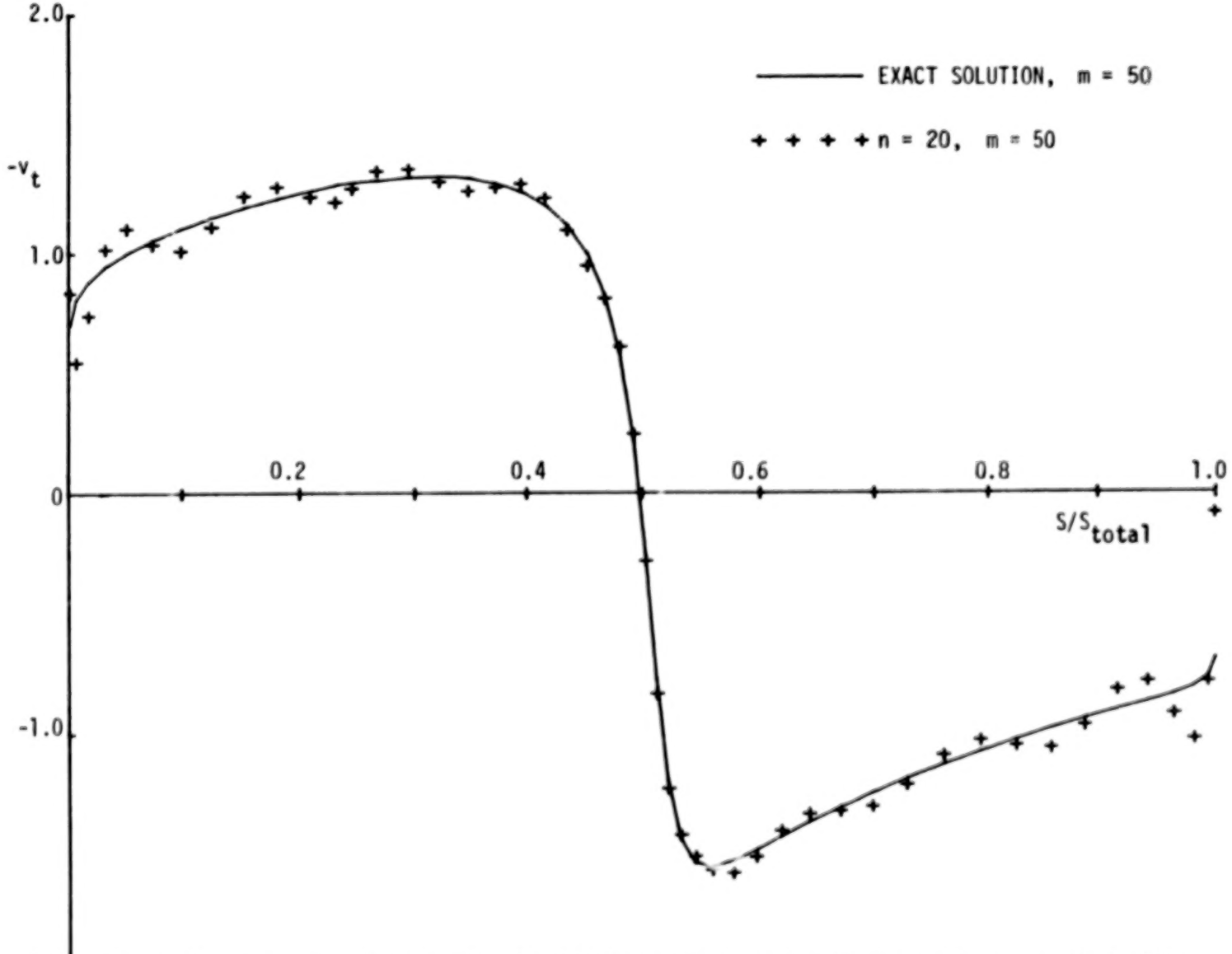

Figure 37. Velocity distribution for BCC#2 nonlifting airfoil; basic Fourier method with Green's identity formulation.

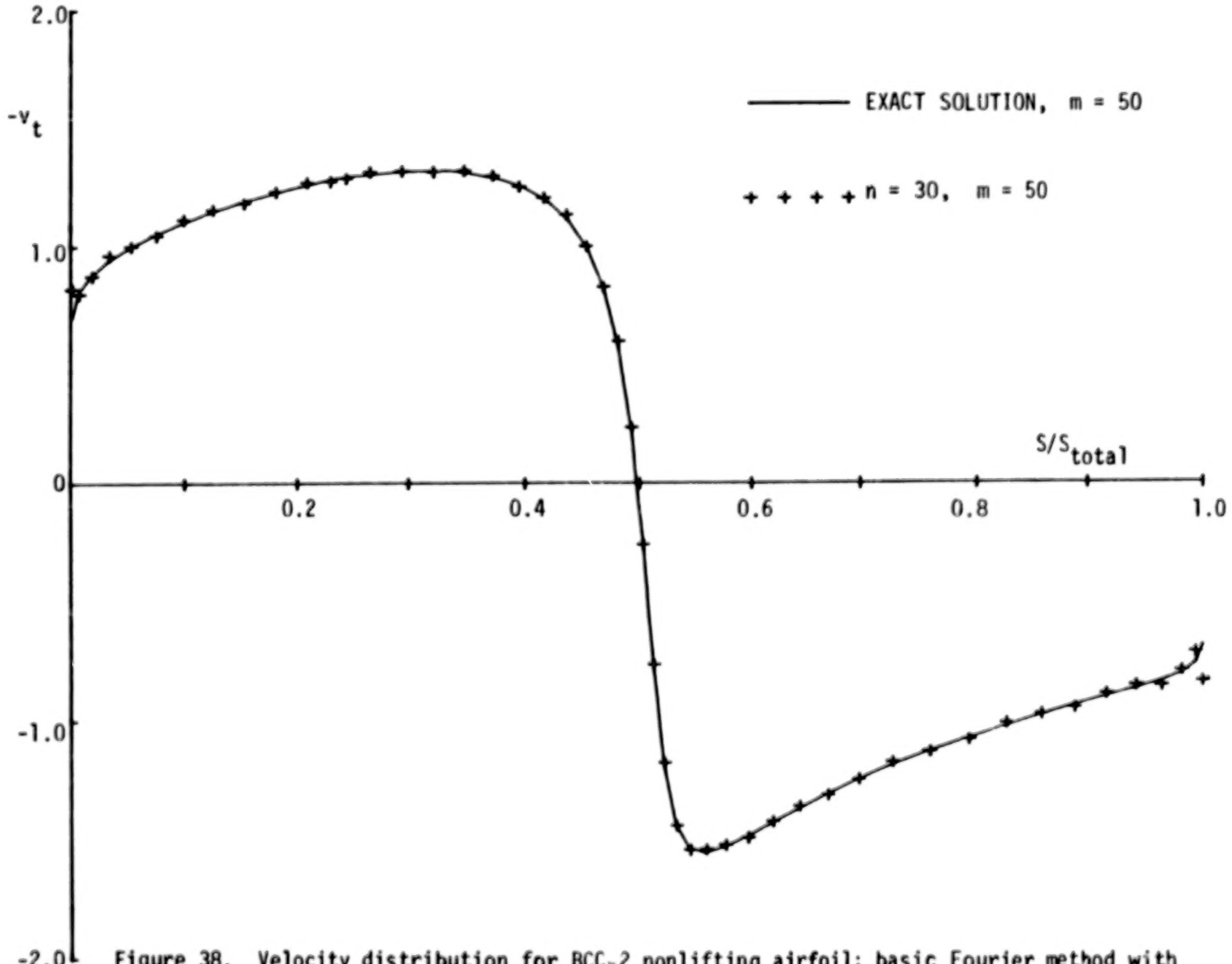

Figure 38. Velocity distribution for BCC$_n$2 nonlifting airfoil; basic Fourier method with Green's identity formulation.

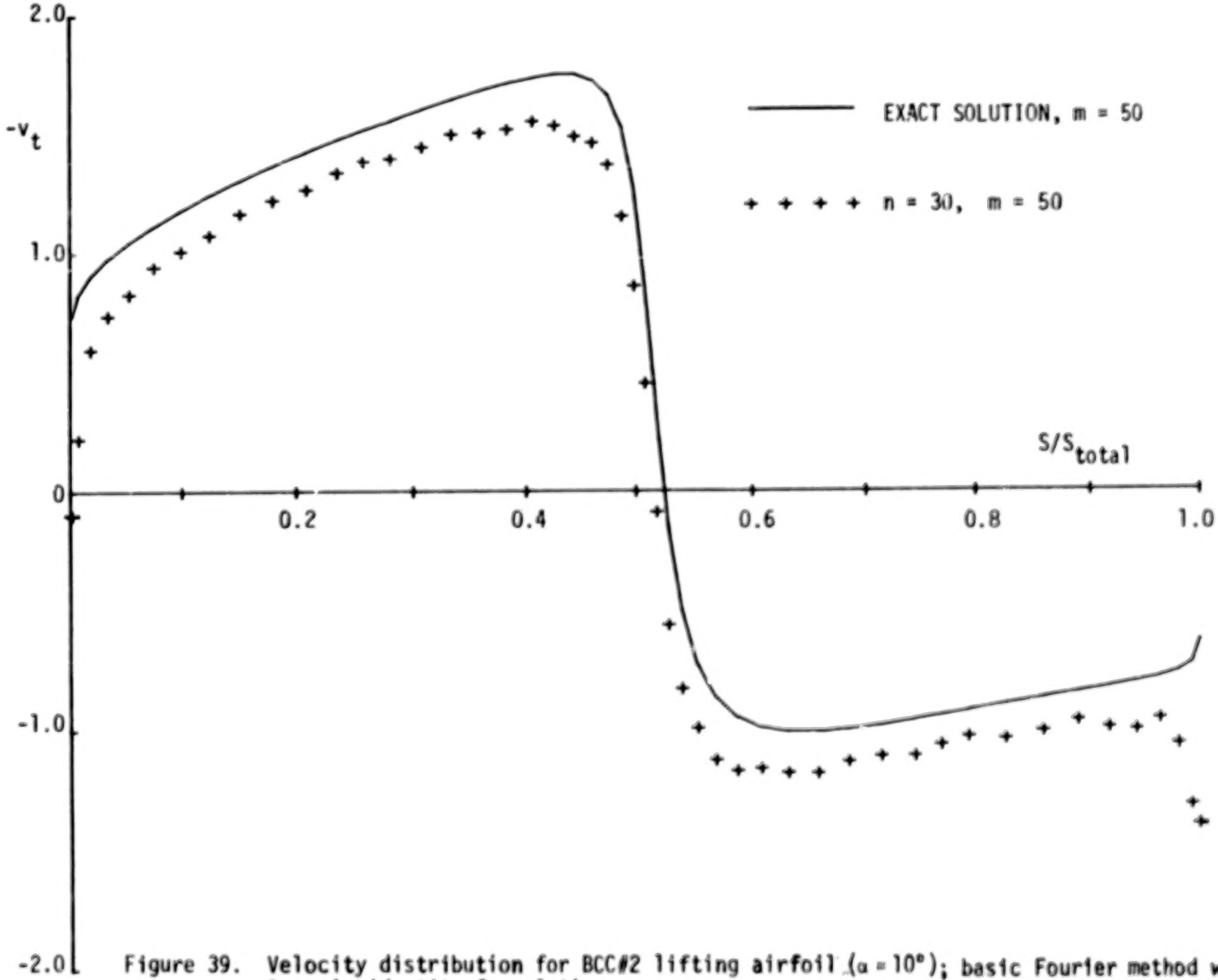

Figure 39. Velocity distribution for BCC#2 lifting airfoil ($\alpha = 10°$); basic Fourier method with Green's identity formulation.

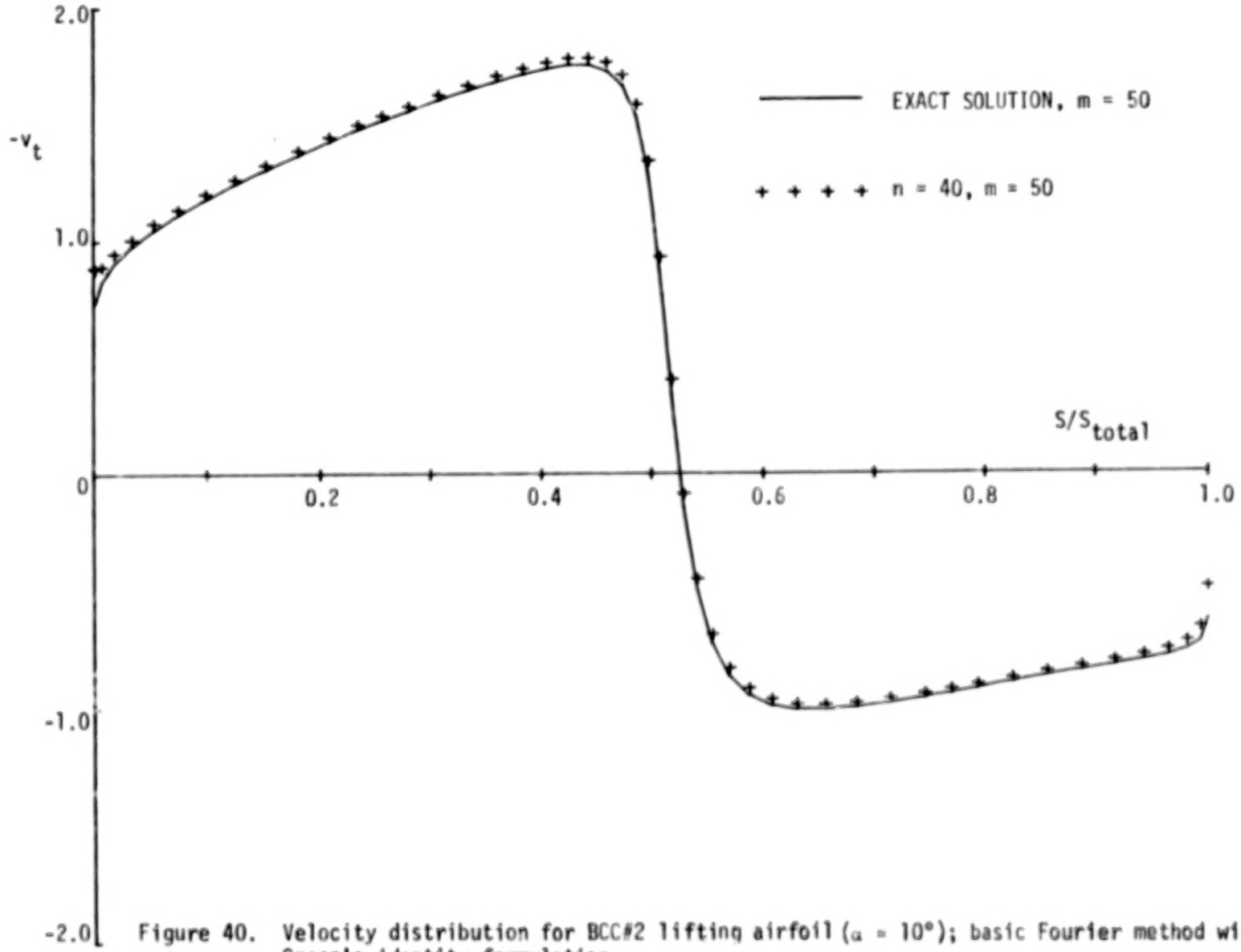

Figure 40. Velocity distribution for BCC#2 lifting airfoil (α = 10°); basic Fourier method with Green's identity formulation.

1. Report No.	2. Government Accession No.	3. Recipient's Catalog No.
NASA CR-3173		

4. Title and Subtitle	5. Report Date
A NEW APPROACH TO THE SOLUTION OF LARGE, FULL MATRIX EQUATIONS – A TWO-DIMENSIONAL POTENTIAL FLOW FEASIBILITY STUDY	September 1979
	6. Performing Organization Code

7. Author(s)	8. Performing Organization Report No.
R. M. James and R. W. Clark	

9. Performing Organization Name and Address	10. Work Unit No.
McDonnell Douglas Corporation Douglas Aircraft Company Long Beach, California 90846	505-06-53-03
	11. Contract or Grant No.
	NAS1-14892

12. Sponsoring Agency Name and Address	13. Type of Report and Period Covered
National Aeronautics and Space Administration Washington, DC 20546	Contractor Report
	14. Army Project No.

15. Supplementary Notes

Langley Technical Monitor: Robert P. Weston

Final Report

16. Abstract

This report presents a new approach to the solution of matrix problems resulting from integral equations of mathematical physics. Based on the inherent smoothness in such equations, the problem is reformulated using a set of orthogonal basis vectors, leading to an equivalent coefficient problem which can be of lower order without significantly impairing the accuracy of the solution. This approach has been evaluated using a two-dimensional Neumann problem describing the inviscid, incompressible flow over an airfoil. Two different kinds of mode functions have been investigated, namely eigenfunction series and Fourier series. The method using Fourier series is found to be preferable. It uses all of the coefficients from a Fast Fourier Transform algorithm in an approximate method which exploits the known structure of the transformed coefficient matrix and very promising results for the flow over a realistic airfoil are obtained. The mode-function method is aimed at reducing the computer time for the solution of the equations for large three-dimensional cases. On the basis of the results presented here, an order of magnitude reduction in this computer time can be expected for such problems as compared with the time for a direct matrix solution.

17. Key Words (Suggested by Author(s))	18. Distribution Statement
Matrix solutions Eigenvectors Fourier series Integral equation solutions Mode functions	Unclassified - Unlimited Subject Category 34

19. Security Classif. (of this report)	20. Security Classif. (of this page)	21. No. of Pages	22. Price*
Unclassified	Unclassified	82	$6.00

*For sale by the National Technical Information Service, Springfield, Virginia 22161

NASA-Langley, 19

END